



PERGAMON

Radiation Physics and Chemistry 60 (2001) 577–596

**Radiation Physics
and
Chemistry**

www.elsevier.com/locate/radphyschem

LIRIC 3.2 an updated model for iodine behaviour in the presence of organic impurities

J.C. Wren*, J.M. Ball

AECL, Chalk River Laboratories, Chalk River, Ontario, Canada K0J 1J0

Received 25 May 2000; accepted 7 November 2000

Abstract

Library of iodine reactions in containment (LIRIC) is a comprehensive mechanistic model for the chemical and mass transport behaviour of iodine in containment under postulated nuclear reactor accident conditions. The LIRIC model has successfully simulated the iodine behaviour in experiments performed under conditions relevant to post-accident containment, and some of the results have been published previously. This document describes the latest version of the model, LIRIC 3.2, and presents simulation results of a few integrated tests performed in the Radioiodine Test Facility. © 2001 Atomic Energy of Canada Limited. Published by Elsevier Science Ltd. All rights reserved.

Keywords: ^{131}I ; Nuclear safety; Modelling iodine behaviour; Post-accident releases

1. Introduction

The time-dependent concentration of airborne iodine in the reactor containment building is one of the most important parameters needed to evaluate the potential radiological consequences of a nuclear reactor accident. The parameter is important because of the large inventory of iodine in irradiated nuclear fuel, and the radiological impact to public dose from an airborne emission of volatile ^{131}I species which could be released to the outside atmosphere through containment leakage or controlled venting. The behaviour of iodine under containment accident conditions has thus been the subject of extensive studies for the world-wide nuclear industry, including Atomic Energy of Canada Limited (AECL), for many years. Recent critical reviews on iodine behaviour (Wren et al., 2000a; Sellers, 1986;

Buxton et al., 1988), and references therein, provide a comprehensive technical background on this subject.

The program at AECL on iodine includes intermediate-scale ("all-effects") experiments using the Radioiodine Test Facility¹ (RTF), and bench-scale ("separate effects") experiments on solution chemistry, surface reactions and mitigation options (Wren et al., 1999a, 2000a). One of the products of the program has been a mechanistic iodine chemistry and transport model, library of iodine reactions in containment (LIRIC), designed to predict the time-dependent behaviour of iodine in containment under a variety of reactor

¹The Radioiodine Test Facility contains an intermediate scale (350 dm³) vessel that is able to provide a combination of reaction media (gas phase, aqueous phase and various surfaces) and conditions (pH, temperature, radiation, various initial concentrations and initial speciation of iodine), to simulate a reactor containment building following an accident. The RTF is equipped with on-line sensors and off-line measurement ports enabling various measurements of chemical and physical properties as a function of time. A description of the RTF and test procedures can be found in Wren et al. (1999a).

*Corresponding author. Tel.: +1-613-584-3311; fax: +1-613-584-1220.

E-mail address: wrenc@aecl.ca (J.C. Wren).

accident conditions² (Wren et al., 1997, 1992; Evans et al., 1990; Paquette, 1989).

As new data and new research findings became available over the past several years, the LIRIC model evolved, and now has a much wider range of applicability, and narrower range of uncertainties than the original model. An earlier version of the model (LIRIC 3.0) was shown to be capable of calculating iodine volatility to within a factor of two from irradiated solutions of CsI at various pH values when the pH profile was provided as input. The results of these simulations have been published (Wren et al., 1999b, 2000a, 1997).

Since the last report on the simulations of various RTF tests using LIRIC 3.0, a number of changes have been made to the model. The addition of temperature sensitivities for many of the rate constants in the iodine and water-radiolysis reaction sets resulted in version 3.1. Subsequently, sub-models were added to describe the dissolution of organic compounds from containment paints into the aqueous phase, and their subsequent aqueous-phase radiolytic degradation with concomitant organic iodide formation. These improvements enable LIRIC to simulate iodine behaviour at temperatures other than room temperature and to predict the pH changes and organic iodide formation observed in RTF experiments performed in painted vessels. In addition, since the last complete documentation of the reactions and transfer phenomena within LIRIC (Evans et al., 1990), many of the reaction rate constants in the original version have been changed, some mechanisms have been refined and several new reaction sets have been added. A full description of the model now designated as LIRIC 3.2 is therefore warranted. This document describes LIRIC 3.2, and presents model simulation results of a few integrated tests performed in the Radioiodine Test Facility.

2. LIRIC 3.2

For a given initial pH, temperature, dose rate and iodine speciation and distribution, LIRIC calculates iodine speciation and concentration in the sump water.

²LIRIC models the interconversion of iodine species within and between the aqueous phase (containment sump water), the gas phase (containment atmosphere) and on dry and wet surfaces (containment walls). LIRIC does not explicitly model the behaviour of iodine in the form of aerosols (dry or wet). Mass transport of iodine aerosols is treated separately as part of aerosol transport models. The interconversion of iodine between aerosol and gaseous forms under accident conditions can be conservatively modelled by treating the wet aerosol phase as being the same as the aqueous phase.

in the gas phase, on dry and submerged surfaces, and in condensing films, as a function of time.

Version 3.2 is the third formal release of the research tool and consists of about 200 reactions. The chemical reactions, surface interactions and mass transport processes described in the model, along with their rate constants, are listed in Tables 1–5. The sources for the rate constants are also listed in the tables. The reactions and processes modelled in LIRIC can be categorized into the following chemical reaction sub-models and physical phenomena:

- (a) water-radiolysis reactions (Table 1),
- (b) inorganic iodine reactions, including thermal aqueous iodine reactions and the reactions of iodine with water-radiolysis products in the aqueous phase (Table 2),
- (c) dissolution of organic solvents from painted surfaces in contact with the aqueous phase (Table 5),
- (d) radiolytic decomposition reactions of organic compounds in the aqueous phase (Table 3),
- (e) organic iodide formation and decomposition in the aqueous phase (Table 3),
- (f) reactions of inorganic impurities such as buffers and metal ions with water-radiolysis products (Table 4),
- (g) mass transfer of O₂, H₂, CO₂, I₂ and organic iodides between the aqueous and gas phases (Table 5), and
- (h) surface interactions, including adsorption and desorption of iodine species on surfaces in contact with the aqueous or gas phase, and absorption on condensing water film (Table 5).

Processes (a)–(h) have been identified as the most important factors affecting iodine behaviour in containment under accident conditions (Wren et al., 2000a). A sub-model containing homogeneous gas-phase reactions of iodine has also been developed (Sagert, 1989), and could easily be incorporated into LIRIC. However, the gas-phase reactions are not considered to be significant contributors to iodine behaviour under accident conditions, thus are not included in LIRIC 3.2. The reaction sets listed above are sufficient to simulate numerous RTF tests performed over a wide range of initial conditions, and to date, there is no evidence that any other processes or phenomenon will have a significant effect on iodine behaviour. The sub-models in LIRIC 3.2 are described in detail in Sections 2.1–2.6.

2.1. Water-radiolysis model

The water-radiolysis sub-model in LIRIC 3.2 (Table 1) contains the primary production reactions of water radiolysis, and the reactions of the primary water-radiolysis products with each other, and with dissolved oxygen. This sub-model contains the reaction set initially compiled by Boyd et al. (1980), with updated

Table 1
Rate constants for water radiolysis used in LIRIC

#	Reactants	Products	Rate constant ^{a,b}	References
1 ^{c,d}	H ₂ O	E ⁻	RAD × (GGE ⁻ + (3.4E-03 × (TCE-25)))	Buxton et al. (1988) and Elliot (1994)
2 ^{c,d}	H ₂ O	•H	RAD × (GGH + (1.28E-03 × (TCE-25)))	Buxton et al. (1988) and Elliot (1994)
3 ^{c,d}	H ₂ O	H ₂	RAD × (GGH ₂ + (0.69E-03 × (TCE-25)))	Buxton et al. (1988) and Elliot (1994)
4 ^{c,d}	H ₂ O	•OH	RAD × (GGOH + (7.17E-03 × (TCE-25)))	Buxton et al. (1988) and Elliot (1994)
5 ^{c,d}	H ₂ O	H ₂ O ₂	RAD × (GGH ₂ O ₂ - (1.49E-03 × (TCE-25)))	Buxton et al. (1988) and Elliot (1994)
6 ^{c,d}	H ₂ O	H ⁻	RAD × (GGH ⁻ + (3.4E-03 × (TCE-25)))	Buxton et al. (1988) and Elliot (1994)
7	e ⁻ + H ₂ O	•H + OH ⁻	1.9 × 10 × EA / (2.2 × 10 ⁷ × 26,000 × TF)	Buxton et al. (1988) and Elliot (1994)
8	e ⁻ + e ⁻ + 2 H ₂ O	OH ⁻ + OH ⁻ + H ₂	5.5E9 × EXP(20,300 × TF)	Buxton et al. (1988) and Elliot (1994)
9	e ⁻ + •H + H ₂ O	OH ⁻ + H ₂	2.5E10 × EXP(15,000 × TF)	Buxton et al. (1988) and Elliot (1994)
10	e ⁻ + H ⁺	•H	2.3E10 × EXP(12,100 × TF)	Buxton et al. (1988) and Elliot (1994)
11	e ⁻ + •OH	OH	3.0E10 × EXP(7900 × TF)	Buxton et al. (1988) and Elliot (1994)
12	e ⁻ + O ₂	•O ₂	1.8E10 × EXP(14,000 × TF)	Buxton et al. (1988) and Elliot (1994)
13	e ⁻ + H ₂ O ₂	•OH + OH	1.4E10 × EXP(15,360 × TF)	Elliot (1994)
14	e ⁻ + •O ₂ + H ₂ O	OH + HO ₂	1.3E10 × EXP(1360 × TF)	Buxton et al. (1988) and Elliot (1994)
15	e ⁻ + HO ₂	•O + OH	3.5E9 × EXP(15,400 × TF)	Buxton et al. (1988) and Elliot (1994)
16	e ⁻ + •O ⁻ + H ₂ O	OH + OH ⁻	2.2E10 × EXP(7900 × TF)	Buxton et al. (1988) and Elliot (1994)
17	•H + •OH	H ₂ O	7.0E9 × EXP(7800 × TF)	Buxton et al. (1988) and Elliot (1994)
18	•H + •H	H ₂	7.75E9 × EXP(15,050 × TF)	Buxton et al. (1988) and Elliot (1994)
19	•H + O ₂	•HO ₂	2.1E10 × EXP(10,610 × TF)	Buxton et al. (1988) and Elliot (1994)
20	•H + •HO ₂	H ₂ O ₂	1.0E10 × EXP(10,600 × TF)	Buxton et al. (1988) and Elliot (1994)
21	•H + H ₂ O ₂	•OH + H ₂ O	9.0E7 × EXP(15,940 × TF)	Buxton et al. (1988) and Elliot (1994)
22	•H + •O ₂	HO ₂ ⁻	2.0E10 × EXP(10,600 × TF)	Boyd et al. (1980) and Elliot (1994)
23	•OH + •O ₂	O ₂ + OH	8.0E9 × EXP(10,850 × TF)	Buxton et al. (1988) and Elliot (1994)
24	•OH + •OH	H ₂ O ₂	5.5E9 × EXP(7650 × TF)	Boyd et al. (1980) and Elliot (1994)
25	•OH + HO ₂	•HO ₂ + OH ⁻	7.5E9 × EXP(15,600 × TF)	Buxton et al. (1988) and Elliot (1994)
26	•OH + H ₂ O ₂	•HO ₂ + H ₂ O	2.7E7 × EXP(15,620 × TF)	Buxton et al. (1988) and Elliot (1994)
27	•OH + H ₂	•H + H ₂ O	4.2E7 × EXP(18,150 × TF)	Buxton et al. (1988) and Elliot (1994)
28	•OH + •HO ₂	O ₂ + H ₂ O	6.0E9 × (5600 × TF)	Buxton et al. (1988) and Elliot (1994)
29	•O ⁻ + •OH	HO ₂	2.0E10 × EXP(7700 × TF)	Buxton et al. (1988) and Elliot (1994)
30	H ₂ O ₂ + •O ⁻	•O ₂ ⁻ + H ₂ O	2.0E8 × EXP(15,600 × TF)	Elliot et al. (1990)
31	H ₂ + •O	•H + OH	8.0E7 × EXP(13,800 × TF)	Buxton et al. (1988) and Elliot et al. (1990)
32	•O ⁻ + HO ₂	OH + •O ₂ ⁻	4.0E8 × EA	Buxton et al. (1988) and Elliot et al. (1990)
33	•O + O ₂	•O ₃ ⁻	3.0E9 × EXP(11,200 × TF)	Boyd et al. (1980) and Elliot (1994)
34	•O ₃	•O ⁻ + O ₂	3.0E2 × EXP(45,700 × TF)	Boyd et al. (1980)
35	•O ₃ + H ₂ O ₂	•O ₂ ⁻ + O ₂ + H ₂ O	1.6E6 × EA	Boyd et al. (1980)
36	•O ₃ + HO ₂	•O ₂ + O ₂ + OH	8.9E5 × EA	Boyd et al. (1980)
37	•O ₃ + H ₂	O ₂ + •H + OH	2.5E5 × EA	Boyd et al. (1980)
38	•HO ₂ + •O ₂	O ₂ + •HO ₂	8.9E7 × EA	Boyd et al. (1980)
39	•HO ₂ + •HO ₂	H ₂ O ₂ + O ₂	2.0E6 × EA	Boyd et al. (1980)
40	H ₂ O ₂	H ⁺ + HO ₂ ⁻	3.56E-2 × EA	Boyd et al. (1980)
41	H ⁺ + HO ₂ ⁻	H ₂ O ₂	2.0E10	Boyd et al. (1980)
42	•HO ₂	H ⁺ + •O ₂ ⁻	8E5 × EA	Boyd et al. (1980)
43	H ⁺ + •O ₂ ⁻	•HO ₂	4.5E10	Boyd et al. (1980)
44	•OH + OH ⁻	•O ⁻ + H ₂ O	1.2E10 × EA	Boyd et al. (1980)
45	•O ⁻ + H ₂ O	•OH + OH ⁻	1.7E6 × EA	Boyd et al. (1980)
46 ^e	H ₂ O	H ⁺ + OH ⁻	k _{46f} - k _{46b} K _w , k _{46b} - 1.43E11	CRC

^aRate constants for forward reactions unless specified. H₂O is included in the reactions only for chemical balance and should not be included in rate equations. The reactions involving H₂O should be treated as unimolecular reactions.

^bT = temperature in Kelvin. TCE = temperature in °C. TF = (1/298.15 - 1/T)/8.314. EA = EXP(18,800 × TF) where 18,800 is the estimated activation energy in J mol⁻¹.

^cGG is the G-value for: H₂O + γ → •OH(2.7), E⁻(2.6), H⁻(2.6), H•(0.6), H₂(0.45), H₂O₂(0.7), where the G-values in parentheses are for the primary production of the species from γ-radiolysis of water at 25 °C (molecules × 100 eV⁻¹).

^dRAD is the dose rate. RAD = (DRATE × 6.242E22)/(3600 × 6.022E25), where DRATE is the dose rate in Mrad h⁻¹.

^eK_w is the dissociation constant of water, and D_w is the density of water where

$$K_w = \text{EXP}_{10}(-4.098 - 3245.5/T + 2.2362E5/(T)^2 - 3.984E7/(T)^3 + (13.957 - 1262.3/T + 8.5641/(T)^2) \times \log(D_w)), \text{ and}$$

$$D_w = 1.00017 - 2.36582E - 5TCE - 4.77122E - 6(TCE)^2 + 8.27411E - 9(TCE)^3.$$

Table 2
Rate constants for reaction of iodine species with water-radiolysis species used in LIRIC

#	Reactants	Products	Rate constant ^{a,b}	References
1 ^c	$I_2 + OH^-$	I_2OH^-	$k_{1f} = 1.0E10$, $k_{1b} = k_{1f}/(K_1/(K_w \times K_2))$ $K_1 = \text{EXP}_{10}(13.880/T - 0.2443 \times T + 308.4)$ $\times \log(T) - 749.1)$	Palmer (1986) Burns et al. (1990)
2	I_2OH^-	$HOI + I^-$	$k_{2f} = 1.3E6$, $k_{2b} = k_{2f}/K_2$, $K_2 = 3 \times 10^{-3} \text{ mol dm}^{-3}$	Lengeyel et al. (1994)
3	$HOI + HOI$	$HIO_2 + H^+ + I^-$	$k_{3f} = 6$, $k_{3b} = 1.7E10$	Wren et al. (1986)
4	$HOI + IO^-$	$IO_2^- + II^+ + I^-$	10	Wren et al. (1986)
5	$IO^- + IO^-$	$IO_2^- + I^-$	2.4E-2	Wren et al. (1986)
6	$I_2OH^- + IO^-$	$IO_2^- + H^+ + 2I^-$	5.25	Wren et al. (1986)
7	$HIO_2 + HOI$	$IO_3^- + 2H^+ + I^-$	$k_{7f} = 240$, $k_{7b} = 5.8E - 1$	Furrow (1987)
8	$IO_2^- + IO^-$	$IO_3^- + I^-$	0.01	Wren et al. (1986)
9	$IO_2^- + I_2OH^-$	$IO_3^- + H^+ + 2I^-$	25	Wren et al. (1986)
10	$HOI + HIO_2 + I^-$	$2HOI + IO^-$	1.8E12	Palmer and Lyons (1989)
11	HIO_2	$IO_2^- + H^+$	$k_{11f} = 1.0E1$, $k_{11b} = 1.0E11$	Estimate
12	$I_2 + I^-$	I_3^-	$k_{12f} = 1E10$, $k_{12b} = k_{12f}/K_{12}$ $K_{12} = D_w \times \text{EXP}_{10}(29688/T + 81.840)$ $\times \log(T) - 0.089649 \times T - 2.0468E6/(T^2) - 526.75)$	Palmer et al. (1984)
13	HOI	$IO^- + H^+$	$k_{13f} = k_{13b} \times K_{13}$, $k_{13b} = 1E10$, $K_{13} = (1/D_w)$ $\times \text{EXP}_{10}(555/T + 7.355 - 2.575 \times \log(T))$	Buxton and Sellers (1985)
14	$\cdot I + e^-$	I^-	$2.4E10 \times EA$	Vinson (1978)
15	$I_2 + e^-$	$\cdot I_2^-$	$5.1E10 \times EA$	Vinson (1978)
16	$IO_3^- + e^-$	$\cdot IO_3^-$	$5.5E9 \times EA$	Dainton and Sills (1962)
17	$\cdot I_2^- + e^-$	$I^- + I^-$	$1.3E10 \times EA$	Sellers (1986)
18	$e^- + I_3^-$	$I^- + \cdot I_2^-$	$3.5E10 \times EA$	Sellers (1986)
19	$\cdot HOI + e^-$	$I^- + OH^-$	$1.9E10 \times EA$	Buxton and Sellers (1985)
20	$\cdot I + \cdot H$	$H^+ + I^-$	$2.7E10 \times EA$	Buxton and Sellers (1985)
21	$I_2 + \cdot H$	$\cdot I_2 + II^+$	$3.5E10 \times EA$	Ishigure et al. (1986)
22	$\cdot I_2^- + \cdot H$	$2I^- + H^+$	$1.8E7 \times \text{EXP}(22.200 \times TF)$	Sellers (1986)
23	$I_3^- + \cdot H$	$I^- + \cdot I_2^- + H^+$	$8.0E9 \times EA$	Sellers, 1986
24	$\cdot H + I^-$	$\cdot HI^-$	$2.5E8 \times \text{EXP}(1800 \times TF)$	Mezyk and Bartels (1993)
25	$\cdot HOI + \cdot H$	$I^- + H_2O$	$4.4E10 \times EA$	Vinson (1978)
26	$IO_2^- + \cdot O_2^- + H_2O$	$IO^- + 2OH^- + O_2$	$1.0E7 \times EA$	Sellers (1986)
27	$I_2 + \cdot O_2^-$	$\cdot I_2 + O_2$	$1.6E12 \times \text{EXP}(-1662/T)$	Schwarz and Bielski (1986)
28	$HOI + \cdot O_2^-$	$OH^- + \cdot I + O_2$	$1.0E6 \times EA$	Buxton and Sellers (1985)
29	$I_3^- + \cdot O_2^-$	$O_2 + I^- + \cdot I_2^-$	$1E12 \times \text{EXP}(-2467/T)$	Schwarz and Bielski (1986)
30	$\cdot I_2^- + \cdot O_2^-$	$O_2 + 2I^-$	$3.0E9 \times EA$	Buxton and Sellers (1985)
31	$\cdot IO + \cdot O_2^-$	$IO^- + O_2$	$8.0E7 \times EA$	Sellers (1986)
32	$\cdot IO + \cdot O_2^- + H_2O$	$HOI + O_2 + OH^-$	1.E9	Paquette (1989)
33	$IO_3^- + \cdot O_2^-$	$\cdot IO_3^- + O_2$	$8.0E9 \times EA$	Estimate
34	$IO_3^- + \cdot O_2^- + H_2O$	$\cdot HIO_3^- + O_2 + OH^-$	5.0E4	Paquette (1989)
35	$\cdot HO_2 + \cdot I_2^-$	$I_2 + HO_2^-$	$1E10 \times EA$	Buxton and Sellers (1985)
36	$HOI + \cdot HO_2$	$O_2 + \cdot I + H_2O$	$1E5 \times EA$	Schwarz and Bielski (1986)
37	$IO_2^- + \cdot HO_2$	$\cdot IO + OH^- + O_2$	$1.E7 \times EA$	Burns and Sims (1989)
38	$\cdot HO_2 + I_2$	$H^+ + O_2 + \cdot I_2^-$	$1.8E7 \times EA$	Schwarz and Bielski (1986)
39	$\cdot I + \cdot OH$	HOI	$1.6E10 \times EA$	Burns (1985)
40	$HOI + \cdot OH$	$\cdot IO + H_2O$	$7E9 \times EA$	Lin (1980)
41	$\cdot IO + \cdot OH$	$III O_2$	$1E10 \times EA$	Lin (1980)
42	$\cdot IO_2 + \cdot OH$	$H^+ + IO_3^-$	$1E10 \times EA$	Lin (1980)
43	$I^- + \cdot OH$	$\cdot HOI^-$	$k_{43f} = 1.1E10 \times EA$, $k_{43b} = 1.13E6 \times EA$	Buxton et al. (1988)
44	$I_2 + \cdot OH$	$HOI + \cdot I$	$1.1E10 \times EA$	Sellers (1986)
45	$IO_3^- + \cdot OH$	$\cdot IO_3 + OH^-$	$1.0E5 \times EA$	Mezyk (1996)
46	$\cdot HOI + \cdot OH$	$OH^- + HOI$	$2.7E10 \times EA$	Vinson (1978)
47	$\cdot HIO_3 + \cdot OH$	$IO_3^- + H_2O$	1.0E9	Sellers (1986)
48	$\cdot I_2^- + \cdot OH$	$I_2 + OH^-$	$3.8E10 \times EA$	Vinson (1978)
49	$\cdot OH + I_3^-$	$OH^- + I_2 + \cdot I$	2E10	Sellers (1986)
50	$I^- + \cdot O^- + H_2O$	$\cdot I + 2OH^-$	$2.6E9 \times EA$	Farhataziz and Ross (1977)
51	$IO^- + \cdot O^- + H_2O$	$\cdot IO + 2OH^-$	$6.0E9 \times EA$	Farhataziz and Ross (1977)

continued opposite

Table 2 (continued)

#	Reactants	Products	Rate constant ^{a,b}	References
52	$\text{IO}_3^- + \cdot\text{OH}^- + \text{H}_2\text{O}$	$\cdot\text{IO}_3 + 2\text{OH}^-$	$2.9\text{E}8 \times \text{EA}$	Farhatiaz and Ross (1977)
53	$\text{I}^- + \text{H}_2\text{O}_2$	$\text{IO}^- + \text{H}_2\text{O}$	$1\text{E}9 \times \text{EXP}(-7424.93/T)$	Burns and Sims (1989)
54	$\text{I}_2\text{OH}^- + \text{H}_2\text{O}_2$	$\text{HIO}_2 + \text{I}^- + \text{H}_2\text{O}$	$k_{54f} = 2.25\text{E}6 \times \text{EXP}(39,000 \times \text{TF})$, $k_{54b} = 1\text{E}7 \times \text{EXP}(101,000 \times \text{TF})$	Ball (2000)
55	$\text{HIO}_2 + \text{OH}$	$\text{I}^- + \text{O}_2 + \text{H}_2\text{O}$	$2.0\text{E}9 \times \text{EXP}(68,000 \times \text{TF})$	Ball (2000)
56	$\cdot\text{IO}_3 + \text{H}_2\text{O}_2$	$\text{H}^+ + \cdot\text{HO}_2 + \text{IO}_3^-$	$1\text{E}9 \times \text{EA}$	Estimate
57	$\cdot\text{I} + \text{H}_2\text{O}_2$	$\cdot\text{HO}_2 - \text{H}^- + \text{I}$	$3.0\text{E}3 \times \text{EA}$	Sellers (1986)
58	$\cdot\text{I} + \text{I}^-$	$\cdot\text{I}_2^-$	$k_{58f} = 1.2\text{E}10 \times \text{EA}$, $k_{58b} = 5.42\text{E}8 \times \text{EXP}(2562/T)$	Sellers (1986)
59	$\cdot\text{HOI}^- + \text{I}^-$	$\cdot\text{I}_2^- + \text{OH}^-$	$2.5\text{E}4 \times \text{EA}$	Sellers (1986)
60	$\cdot\text{HOI}^-$	$\cdot\text{I} + \text{OH}^-$	$1.2\text{E}8 \times \text{EA}$	Sellers (1986)
61	$\text{H}^+ + \text{O}_2 + \cdot\text{I}_2$	$\cdot\text{HO}_2 + \text{I}_2$	$6\text{E}5 \times \text{EA}$	Burns and Sims (1989)
62	$\cdot\text{I}_2 + \cdot\text{I}_2^-$	$\text{I}_3^- + \text{I}$	$4.5\text{E}9 \times \text{EA}$	Sellers (1986)
63	$\cdot\text{I}_2 + \cdot\text{I}$	I_3^-	$5\text{E}9 \times \text{EA}$	Ishigure et al. (1986)
64	$\cdot\text{I} + \cdot\text{I}$	I_2	$1\text{E}10 \times \text{EA}$	Sellers (1986)
65	$\text{HOI}^- + \cdot\text{I}_2^-$	$2\text{I}^- + \cdot\text{IO} + \text{H}^-$	$1\text{E}5 \times \text{EA}$	Buxton and Sellers (1982)
66	$\cdot\text{IO}_3^- + \text{H}_2\text{O}$	$\cdot\text{HIO}_3^- + \text{OH}^-$	$5.5\text{E}9 \times \text{EA}$	Buxton and Sellers (1985)
67	$\cdot\text{IO}_3 + \text{I}^-$	$\text{IO}_2^- + \cdot\text{IO}$	$1\text{E}4 \times \text{EA}$	Estimate
68	$\cdot\text{IO}_2 + \text{I}^-$	$\text{I}_2 + \cdot\text{O}_2^-$	$1\text{E}10 \times \text{EA}$	Estimate
69	$\cdot\text{HI}^- + \text{H}_2\text{O}$	$\text{H}_2 + \text{OH}^- + \cdot\text{I}$	$1.3\text{E}3 \times \text{EA}$	Sellers (1986)
70	$\text{H}^+ + \cdot\text{HI}^-$	$\text{H}_2 + \cdot\text{I}$	$1\text{E}10 \times \text{EA}$	Sellers (1986)
71	$\cdot\text{I}_2 + \cdot\text{HOI}^-$	$\text{I}_3^- + \text{OH}^-$	$1.8\text{E}10 \times \text{EA}$	Palmer et al. (1984)
72	$\cdot\text{HOI}^- + \cdot\text{I}$	$\text{I}_2 + \text{OH}^-$	$2.3\text{E}10 \times \text{EA}$	Palmer et al. (1984)
73	$\cdot\text{HOI}^- + \cdot\text{HOI}^-$	$\text{I}_2 + 2\text{OH}^-$	$2.0\text{E}10 \times \text{EA}$	Sellers (1986)
74	$\cdot\text{IO}^- + \cdot\text{IO}$	I_2O_2	$1.5\text{E}9 \times \text{EA}$	Buxton and Sellers (1985)
75	$\text{I}_2\text{O}_2 + \text{H}_2\text{O}$	$\text{IO}_2^- + \text{HOI} + \text{H}^+$	$k_{75f} = 1\text{E}10$, $k_{75b} = 1.0\text{E}7 \times \text{EA}$	Buxton and Sellers (1985)
76	$\cdot\text{IO} + \text{IO}_2^-$	$\cdot\text{IO}_2 + \text{IO}^-$	$1\text{E}10 \times \text{EA}$	Buxton and Sellers (1985)
77	$\cdot\text{IO}_2 + \text{H}_2\text{O}$	$\cdot\text{HIO}_3^- + \text{H}^+$	$5.5\text{E}4 \times \text{EA}$	Buxton and Sellers (1985)
78	$2\cdot\text{HIO}_3$	$\text{IO}_3 + \text{IO}_2^-$	$k_{78f} = 1\text{E}10$, $k_{78b} = 100 \times \text{EA}$	Buxton and Sellers (1985)

^a Rate constants for forward reactions unless specified. The units are $\text{dm}^3 \text{mol}^{-1} \text{s}^{-1}$ for bimolecular (second-order) reactions, and s^{-1} for unimolecular (first-order) reactions. The reactions involving H_2O should be treated as unimolecular reactions.

^b T = temperature in Kelvin, TCE = temperature in °C, $\text{TF} = (1/298.15 - 1/T)/8.314$, $\text{EA} = \text{EXP}(18,800 \times \text{TF})$ where 18,800 is the estimated activation energy in J mol^{-1} .

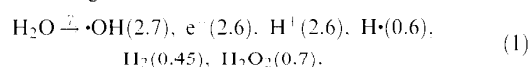
^c K_1 is the equilibrium constant of reaction, $\text{I}_2 + \text{H}_2\text{O} = \text{HOI} + \text{I}^- + \text{H}^+$, where $K_1 = \text{EXP}_{10}(13,880/T - 0.2445 \times T + 308.4 \times \log(T) - 749.1)$.

^d K_w is the dissociation constant of water (see footnote e of Table 1).

^e $K_2 = k_{2f}/k_{2b}$, where $K_2 = 3 \times 10^{-3} \text{mol dm}^{-3}$.

primary G -values and reaction rates reported by Buxton et al. (1988) and Elliot et al. (1990), Elliot (1994).

The primary water-radiolysis products are formed according to



where the numbers in parentheses are the G -values (molecules $\times (100 \text{eV})^{-1}$) for the production of the species from the γ -radiolysis of water at 25 °C (Buxton et al., 1988). For a given radiation dose, the G -values provide the zeroth-order rate constants for the formation of these species. The temperature dependence (or Arrhenius parameters) of the G -values incorporated into LIRIC 3.2 were based on recent experimental work (Elliot, 1994).

The primary production reactions shown above, along with Boyd's compilation of reactions of the

primary water-radiolysis products with each other, and with dissolved oxygen accurately reproduce experimentally observed radiolysis product concentrations from continuous radiolysis experiments over a range of dose rates and temperatures (Christensen and Sehested, 1988; Elliot et al., 1990). The water-radiolysis model, in combination with organic radiolysis reactions, has also been shown to reproduce the product formation from many continuous radiolysis experiments containing organic compounds (Glowa et al., 2000a; Wren and Glowa, 2000).

2.2. Inorganic iodine chemistry

The inorganic iodine sub-model within LIRIC 3.2 contains about 80 reactions covering the formation and interconversion of 15 inorganic iodine species (Table 2).

Table 3
Reactions and rate constants for the simplified organic radiolysis and organic iodide model

Number	Reaction	Rate constant
1 ^a	ORG + ·OH → 6·ORG	1.0E9
2 ^a	·OH →	1.0E9 × 5 · [ORG]
3	·ORG + O ₂ → CO ₂	1.0E9
4	CO ₂ = H ₂ CO ₃	k _f = 0.03, k _b = 20
5	H ₂ CO ₃ = H ⁺ + HCO ₃ ⁻ (pKa = 6.4)	k _f = 2E6, k _b = 1.0E10
6	HCO ₃ ⁻ = H ⁺ + CO ₃ ²⁻ (pKa = 10.3)	k _f = 0.484, k _b = 1.0E10
7	·ORG + I ₂ → LVRI + ·I	6.6E9
8	·ORG + I ₂ → HVRI + ·I	3.3E8
9	·ORG + HOI → LVRI + ·OH	1.5E7
10	·ORG + HOI → HVRI + ·OH	7.0E5
11	LVRI + e ⁻ → I ⁻ + ·ORG	1.0E10
12	HVRI + e ⁻ → I ⁻ + ·ORG	1.0E10
13	LVRI → ORG + I ⁻	1.0E-6 × EXP (1E5/(1/298.15-1/T))/8.314
14	HVRI → ORG + I ⁻	1.0E-6 × EXP (1E5/(1/298.15-1/T))/8.314

^aThe model assumes that the average number of carbons in an organic solvent from containment paints would be 6, and 6 ·ORG represents the sum of several generic intermediate species formed during the radiolysis. The organic radical formation is known to have a first order dependence on ·OH, and thus is expressed as first-order dependent on ·OH in Reaction 1. However, because decomposition of a 6 carbon organic compound to 6 CO₂ molecules would consume 6 ·OH and 6 O₂, Reaction 2 has been added to properly maintain the [·OH] (see text for further discussion).

Table 4
Rate constants for reaction of Fe²⁺/Fe³⁺ with water-radiolysis species used in LIRIC

#	Reactants	Products	Rate constant ^{a,b}	References
1	Fe ²⁺ + ·OH	Fe ³⁺ + OH ⁻	3.0E9 × EXP(15,100 × TF)	Sellers (1986)
2	Fe ³⁺ + ·O ₂ ⁻	Fe ²⁺ + O ₂	k _f = 1.5E8 × EXP(15,100 × TF), k _b = 1E9	Sellers (1986)
3	Fe ²⁺ + H ₂ O ₂	Fe ³⁺ + ·OH + OH ⁻	55 × EXP(85,210 × TF)	Sellers (1986)
4	Fe ³⁺ + ·H	Fe ²⁺ + H ⁺	1.0E8 × EXP(22,200 × TF)	Sellers (1986)
5	Fe ³⁺ + e ⁻	Fe ²⁺	6.0E1 × EXP(15,100 × TF)	Sellers (1986)
6	Fe ²⁺ + ·O ₂	Fe ³⁺ + HO ₂ ⁻ + OH ⁻	1.0E7 × EXP(15,100 × TF)	Sellers (1986)

^a Rate constants for forward reactions unless specified. The units are dm³ mol⁻¹ s⁻¹ for second-order reactions, and s⁻¹ for first-order reactions.

^b TF = (1/298.15 - 1/T)/8.314, where T = temperature in Kelvin.

The model consists of reactions of iodine species with water-radiolysis products, thermal reactions for the oxidation of iodide and the disproportionation of HOI, and radiolytic and thermal reactions for formation and depletion of iodate. Rate constants, equilibrium constants and Arrhenius parameters for each of the reactions in the model were obtained from experimental studies either reported in the literature or measured in our own laboratories (see Table 2 for individual references).

Although it is difficult to unequivocally verify some of the mechanisms or rate constants in the model, the most important ones for reactor accident analysis, and therefore those that require the most accuracy in their rate constants, are well known, and their rate constants are well established. These are

- (a) the oxidation of I⁻ by the primary water-radiolysis product, ·OH, to molecular iodine, I₂, via Reactions 43, 60, 58, 62, 63, 64 and 12 in Table 2, whose

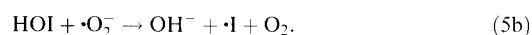
overall reaction can be expressed as



- (b) the hydrolysis of molecular iodine, via Reactions 1, 2 and 13 in Table 2;



- (c) the reduction of I₂ and its hydrolysis products to I⁻ by water-radiolysis products H₂O₂ and O₂⁻, via Reactions 54, 55, 27 and 28 in Table 2;



The key reactions, and the reactions required for the mass balance for key reactants (mainly ·OH), are

Table 5
Equations used to describe transport phenomenon

#	Phenomenon	Rate equation
(1)	Dissolution of organic solvents from paints	$\frac{d[\text{ORG}(\text{aq})]}{dt} = k_{\text{DIS}}([\text{ORG}(\text{aq})]_{\infty} - [\text{ORG}(\text{aq})])$
(2) ^{a, d}	Mass transfer between the liquid and gas phase	$\frac{d([\text{VOLI}(\text{g})])}{dt} = k_{\text{MT}} \frac{A_{\text{int}}}{V_{\text{g}}}([\text{VOLI}(\text{aq})] - ([\text{VOLI}(\text{g})]H_{\text{VOLI}}))$ $\frac{d([\text{VOLI}(\text{aq})])}{dt} = k_{\text{MT}} \frac{A_{\text{int}}}{V_{\text{aq}}}([\text{VOLI}(\text{g})]H_{\text{VOLI}} - ([\text{VOLI}(\text{aq})])$
(3) ^{d, f}	Adsorption on gas-phase surfaces	$\frac{d([I_2(\text{g})])}{dt} = -k_{\text{AD}}[I_2(\text{g})] \left(1 - \frac{[I(\text{ad})]}{\text{SAT}}\right)$ $\frac{d([I(\text{ad})])}{dt} = k_{\text{AD}} \frac{V_{\text{g}}}{A_{\text{g}}} [I_2(\text{g})] \left(1 - \frac{[I(\text{ad})]}{\text{SAT}}\right)$
(4) ^{d, f}	Desorption from gas phase surfaces	$\frac{d([I_2(\text{g})])}{dt} = k_{\text{DES}} \frac{A_{\text{g}}}{V_{\text{g}}} [I(\text{ad})]$ $\frac{d([I(\text{ad})])}{dt} = -k_{\text{DES}} [I(\text{ad})]$
(5) ^{g, h}	Adsorption of iodine into condensate	$\frac{d([I(\text{con})])}{dt} = k_{\text{AD}}^{\text{cw}} [I_2(\text{g})] \frac{V_{\text{g}}}{V_{\text{con}}}$ $\frac{d([I_2(\text{g})])}{dt} = -k_{\text{AD}}^{\text{cw}} [I_2(\text{g})]$
(6) ^{g, i}	Removal of iodine from condensate to bulk phase	$\frac{d([I(\text{con})])}{dt} = -k_{\text{con}} [I(\text{con})]$ $\frac{d([\text{NONVOLI}(\text{aq})])}{dt} = k_{\text{con}} [I(\text{con})] \frac{V_{\text{con}}}{V_{\text{aq}}}$

^a [VOLI(g)] and [VOLI(aq)] are volatile iodine species (I₂, HVRI, LVRI) concentrations in the gas and aqueous phase (mol dm⁻³). The same description is also used for other volatile species (e.g., CO₂, O₂ and H₂).

^b *H* is the ratio of the concentration of a species in the liquid phase to the gas phase at equilibrium (dimensionless).

^c *k*_{MT} is the overall mass transfer coefficient (dm s⁻¹), 1/*k*_{MT} = 1/*k*_l + *H*/*k*_g, where *k*_l and *k*_g are the liquid- and gas-phase mass transfer coefficients, respectively, and *H* is the partition coefficient of the species.

^d *A*_{int} is the interfacial mass transfer surface area (dm²), *A*_g is the dry surface area (dm²), and *V*_g and *V*_{aq} are the volumes of gas and aqueous solution (dm³).

^e [I(ad)] and [I⁻(con)] are iodine species retained on dry surfaces (mol dm⁻²) and in the condensate (mol dm⁻³).

^f *k*_{AD} is the adsorption rate constant (s⁻¹), *k*_{DES} is the desorption rate constant (s⁻¹), and [SAT]_g is the saturation capacity of the surface for I₂ (mol dm⁻²).

^g *k*_{AD}^{cw} is the adsorption rate constant on condensing water film (s⁻¹).

^h *A*_{con} and *V*_{con} are the surface area (dm²), and volume (dm³) of the condensate, respectively.

ⁱ *k*_{con} = *F*_{con}/*V*_{con} where *F*_{con} is the volume flow rate of the condensate.

highlighted in bold in Table 2. This reduced reaction set forms the basis of the reduced inorganic iodine sub-model incorporated into the next version of LIRIC described in detail elsewhere (Ball, 2000).

The overall oxidation, Reactions (2a) and (2b), are responsible for the conversion of non-volatile iodide to volatile iodine species, whereas Reactions (3)–(5) are the main pathways for conversion of volatile iodine to non-volatile iodine species, and are responsible for the strong pH dependence of iodine volatility (Wren et al., 1999a, 2000a). Rate constants measured for the forward reaction of Reaction 43 in Table 2, which is the rate determining step for the overall oxidation process (a), are in reasonably good agreement with one another, ranging from 0.9 × 10¹⁰ to 1.8 × 10¹⁰ dm³ mol⁻¹ s⁻¹ (Buxton et al., 1988; Ishigure et al., 1986; Elliot, 1992). Likewise, the overall equilibrium constant for iodine

hydrolysis Reaction (3) (I₂ + H₂O = HOI + I⁻ + H⁺) and its temperature dependence is reasonably well established (Wren et al., 1986; Sellers, 1986; Burns et al., 1990). The overall equilibrium constant reported by Burns et al. (1990) has been incorporated in the rates of Reaction 1 in Table 2.

Rate constants for the iodine reduction by H₂O₂, Reactions 54 and 55 in Table 2, have been measured in our laboratories as a function of pH, temperature, iodide concentration, H₂O₂ concentration, and with various buffers (Ball et al., 1997a; Ball and Hnatiw, 2000). Rate constant determinations made at room temperature with citrate and phosphate buffer compare well (within 20%) to those obtained in other studies (Liebhafsky, 1932; Shiraishi et al., 1992; Kassai-Rabia et al., 1993). The temperature dependence of the reaction is also similar to that measured under more

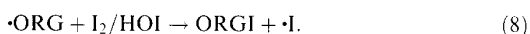
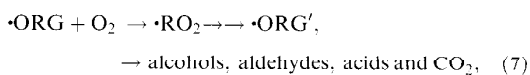
limited conditions by Liebhafsky (1935). Therefore, the reaction rate constants are considered to be well determined.

The rate constant for Reaction (5a), or Reaction 27 in Table 2, has been measured by Schwarz and Bielski (1986) over a wide range of pH values. Schwarz's rate constant agrees well with an indirect determination of the constant performed at room temperature in neutral solution (Ishigure et al., 1986). Because Reaction (5a) is an electron transfer reaction, it is fast at room temperature, and has a relatively small-temperature dependence. An activation energy of 27 kJ mol^{-1} was determined by Schwarz and Bielski (1986) for the reaction. The rate constant for Reaction 28 in Table 2 is that of Buxton and Sellers (1985) and in agreement with the estimate of the value given by Schwarz and Bielski (1986).

2.3. The effect of organic impurities

As discussed in Section 2.2, hydrolysis of volatile I_2 to non-volatile HOI and I^- , and reduction of volatile I_2 by $\cdot\text{O}_2^-$ and H_2O_2 to I^- are pH-sensitive processes. It is for this reason that pH has a dramatic effect on iodine volatility, and that predicting changes in aqueous pH is crucial to modelling iodine behaviour.

Experimental studies have established that, in the presence of a radiation field, iodine behaviour is very dependent upon the presence of organic impurities in the aqueous phase (Ball et al., 1997b; Wren et al., 1999a; Wren et al., 1999b). These impurities can change the pH and the redox characteristics (i.e., $\cdot\text{OH}$, $\cdot\text{O}_2^-$ and H_2O_2 concentrations) of an aqueous solution via Reactions (6) and (7), and can react with molecular iodine to form organic iodides via Reaction (8) (Wren et al., 1999a, 2000a).



Although there are many different sources of organic material in containment, the organic impurities that would have the most significant impact on iodine volatility are those that would be dissolved in aqueous solutions where they could participate in Reactions (6)–(8). It has been established that the major sources of such impurities would be solvents dissolved from painted surfaces in containment into the containment sump (Wren et al., 1999a, 2000b). Three sub-models have been added to LIRIC to describe the effect of organic impurities derived from containment paints on

pH and iodine behaviour. These sub-models are described in the following sections.

2.3.1. Organic dissolution model

A model for the dissolution of organic materials from painted surfaces into the aqueous phase has been incorporated into LIRIC 3.2 (Eq. (1) in Table 5) based on experimental studies on vinyl-, polyurethane-, and epoxy-containment coatings (Ball et al., 2000; Wren et al., 1999a, 2000b). When these surfaces come in contact with water, organic solvents trapped in the paint polymer phase (e.g., thinners such as toluene, xylene, MIBK and MEK) are "leached" into the aqueous phase. The concentration of organic solvent in aqueous solution at time t , $[\text{ORG}(\text{aq})]_t$, can be described by a first-order kinetic equation (Wren et al., 1999a,b, 2000b):

$$[\text{ORG}(\text{aq})]_t \propto [\text{ORG}(\text{aq})]_\infty (1 - \exp(-k_{\text{DIS}}t)), \quad (9)$$

where $[\text{ORG}(\text{aq})]_t$ and $[\text{ORG}(\text{aq})]_\infty$ represent the amount of organic compound at time t , and at time ∞ (infinitely long time periods) in the aqueous phase, respectively, k_{DIS} is the dissolution rate constant (s^{-1}) and $[\text{ORG}(\text{aq})]_\infty$ (mol dm^{-3}) is determined by the amount of solvent in the paint polymer phase available to be released into a given volume of water.

The dissolution kinetics of many common solvents from a variety of different types of paints followed the same mechanism, with approximately the same dissolution rate constant for a given coating thickness. The rate constant k_{DIS} was found to be independent of the aqueous pH, and insensitive to the effects of radiation, but dependent upon temperature, with an activation energy ranging from 50 to 100 kJ mol^{-1} for the four paint types studied (Wren et al., 2000b). The rate constant was also inversely proportional to paint coating thickness (i.e., $k_{\text{DIS}} \propto 1/L$), indicating that solvent release is a diffusion process (Ball et al., 2000).

The total concentration of organic solvent in the aqueous phase at the end of dissolution, $[\text{ORG}(\text{aq})]_\infty$, depends on the coating thickness, and the paint surface area to water volume ratio. It also depends on the age of the coating, implying the organic content in the coating decreases because of evaporative losses. Even after several years, however, there are significant quantities of organic solvents which are available to be released by dissolution (Wren et al., 2000b). The effect of paint aging on the rate constant for solvent release has yet to be established.

Because the dissolution rate constant is independent of the type of paint and the type of organic solvent, and its dependence upon temperature and coating thickness has been established, the dissolution rate constant, k_{DIS} , has been defined within LIRIC 3.2. On the other hand $[\text{ORG}(\text{aq})]_\infty$ is reactor and accident specific and is thus a user defined input in LIRIC 3.2. One of the objectives of

our on-going dissolution studies is also to provide the range of $[\text{ORG}(\text{aq})]_{\infty}$ expected in an accident, which will be dependent upon the initial solvent content of paints and the paint age.

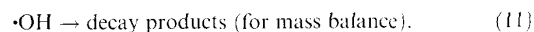
2.3.2. Organic radiolysis model

The radiolytic degradation of organic impurities originated from painted surfaces, Reactions (6) and (7), and associated acid–base equilibria, are described in LIRIC 3.2 using a simplified reaction set, Reactions 1–6 in Table 3. Development of the simple organic radiolysis model for LIRIC began with experimental studies on the radiolytic degradation of methyl ethyl ketone (MEK), a common organic solvent used in paints (Driver et al., 2000). These studies were used to develop a comprehensive mechanistic model consisting of about 110 organic reactions (Glowa et al., 2000a), which reproduced observed MEK decomposition, various radiolysis product concentrations, and the pH changes induced by carboxylic acids and CO_2 formation in the irradiated solutions. A model consisting 110 reactions for the decomposition of one organic compound was not practical for incorporation into LIRIC, particularly since MEK is only one of the many organic solvents that could be released into the sump in containment. Consequently, the full MEK model was simplified to one containing only seven reactions and four equilibria. This model also reproduced the experimentally observed behaviour of MEK and intermediate degradation products, indicating that the key reactions required to model its degradation were well understood (Wren and Glowa, 2000).

Once a sound understanding of the key processes involved in aqueous-phase radiolysis of organic compounds was established, organic radiolysis experiments were expanded to examine decomposition of other organic compounds (methyl isobutyl ketone and toluene) over a wider range of conditions. These included radiation dose rates ranging from 0.4 to 5 kGy h^{-1} , initial organic concentrations ranging from 1×10^{-6} to $1 \times 10^{-3} \text{ mol dm}^{-3}$, and organic injection rates ranging from instantaneous addition to slow and continuous injection to simulate dissolution from painted surfaces. In conjunction with the simplified MEK model, these studies led to the development of a generic organic degradation model applicable to reactor accident conditions (Glowa et al., 2000b).

Unless large quantities of organic material are instantaneously introduced into the containment sump water, the rate of dissolution of organic species into the containment sump water will be the rate determining step for organic radiolysis and organic iodide production. When this is the case, for the purpose of predicting pH and organic radical concentration (required for predicting organic iodide formation), the organic

degradation process can be simplified to



The above model uses an organic molecule containing 6 carbons as the basis for the decomposition scheme, a reasonable assumption in view of a survey showing that the most common and abundant paint solvents contain between 4 (e.g., MEK) and 8 (e.g., xylene, ethyl benzene) carbons (Wren et al., 2000b). The model also assumes, based on the detailed radiolysis studies of MEK (Glowa et al., 2000a; Wren and Glowa, 2000), and subsequent studies of the oxygen consumption during radiolysis of MIBK and toluene (Glowa et al., 2000b), that decomposition of a 6-carbon organic species consumes six $\cdot\text{OH}$ radicals and approximately six O_2 molecules.

It has been also shown that the rate determining step for the radiolytic decomposition of an organic species is its reaction with $\cdot\text{OH}$ and that the overall organic radical formation has a first-order dependence on $\cdot\text{OH}$ concentration (Wren and Glowa, 2000; Glowa et al., 2000b). For this reason, the organic radical formation in LIRIC 3.2 is represented by a reaction, having a first-order dependence on $\cdot\text{OH}$, as shown in Reaction (10), or Reaction 1 in Table 3. However, a mass balance equation for $\cdot\text{OH}$, Reaction (11) or Reaction 2 in Table 3, is incorporated to account for the fact that the overall degradation of one 6-carbon organic compound consumes six moles of $\cdot\text{OH}$, whereas Eq. (10) consumes only one as written. Because the concentration of $\cdot\text{OH}$ is crucial in determining the rate of oxidation of iodine, it is important that the concentration is calculated correctly.

The rate constants used for Reactions 1–3 in Table 3 in LIRIC 3.2 have been chosen as being typical values (based on literature review) for the reactions of organic compounds with $\cdot\text{OH}$ and for the reaction of O_2 with organic radicals (Glowa et al., 2000b). The equilibria involving $\text{CO}_2(\text{aq})$ and its hydrolysis products are also included in the organic radiolysis sub-model, as these species are largely responsible for the pH changes associated with organic radiolytic degradation.

The simple model for organic radiolysis and its associated acid–base equilibria, consisting only of Reactions 1–6 in Table 3, reproduces the results of numerous bench-scale and RTF tests in which organic compounds are introduced gradually into the aqueous phase, either by dissolution from paints or by injection (Glowa et al., 2000b). The organic degradation model still undergoes rigorous testing to determine uncertainties and to ensure that it is robust and flexible with respect to various potential scenarios of organic additions into the sump water in following an accident.

However, the current version of the generic radiolysis model (first six reactions in Table 3), in combination of the organic iodide sub-model discussed in the following section, which has been incorporated into LIRIC 3.2 has been able to simulate pH and organic iodide behaviour observed in the RTF tests performed in painted vessels (see Section 3).

2.3.3. Organic iodide formation and decomposition model

Formation and decomposition of organic iodides are likely to be dominated by aqueous homogeneous processes in post-accident containment, with the predominant formation mechanism being the reaction of molecular iodine and its hydrolysis products with radicals produced from radiolytic decomposition of organic impurities (Reaction (10)) (Wren et al., 1999a, 2000a). However, the type of organic compounds and organic radicals originating from painted surfaces, and, consequently, the type of organic iodides, varies widely. To handle the large number of organic radicals and resulting organic iodide species in a practical manner, the organic iodide behaviour was described by grouping organic iodides into two categories, low volatility organic iodides (LVRI, e.g., iodoacetic acid) and high volatility organic iodides (HVRI, e.g., CH_3I). The organic iodide model incorporated in LIRIC 3.2 (Table 3) consists of a small number of representative reactions:

- (1) formation of low volatility organic iodides (LVRI) from organic radicals and I_2 (and its hydrolysis product, HOI) (Reactions 7 and 9 in Table 3),
- (2) formation of highly volatile organic iodides (HVRI) from organic radicals and I_2 (and its hydrolysis product, HOI) (Reactions 8 and 10 in Table 3),
- (3) radiolytic decomposition of organic iodides by water-radiolysis product, e_{aq}^- , to $\text{R}\cdot$ and I^- , (Reactions 11 and 12 in Table 3),
- (4) hydrolysis of organic iodides forming alcohol and I^- (Reactions 13 and 14 in Table 3), and
- (5) partitioning of LVRI and HVRI between the aqueous and gas phases (Eq. (2) in Table 5).

The grouping of organic iodides into the two, LVRI and HVRI, requires the use of effective rate constants for the processes (1)–(4) and the effective partition coefficients for process (5). LIRIC 3.2 uses effective partition coefficients of 1000 for LVRI and 5 for HVRI (that of CH_3I at 25°C), where the partition coefficient, H , is defined as the ratio of the aqueous-phase to gas-phase concentration of a species at equilibrium (see Section 2.5 for further description of partition coefficient). These values represent weighted averages of a wide range of low volatility and high volatility organic iodides, obtained from extensive literature review (Glowa and Wren, 2001). The partition coefficients, being thermodynamic equilibrium constants, are as-

sumed to follow a simple thermodynamic temperature dependence, where ΔG is equivalent to the free energy of the equilibrium between the aqueous and gas phases. Values for ΔG also represent a weighted average from literature review (Glowa and Wren, 2001):

$$\ln(H_{\text{LVRI}}) = \ln(H_{\text{LVRI}(298\text{ K})}) + (-\Delta G_{\text{HVRI}}/R) \times (1/T - 1/298). \quad (13)$$

The rate constant used in LIRIC for reaction between I_2 and organic radicals (sum of the rate constants for Reactions 7 and 8 in Table 3) is that reported for reaction between $\cdot\text{CH}_3$ and I_2 (Thomas, 1967). This is considered to be a reasonable estimate, because rate constants for such radiolytic processes are, in general, molecular diffusion limited (Poutsma, 1973). Estimates for the rate constants for reaction between HOI and organic radicals (Reactions 9 and 10 in Table 3) were made based on modelling studies performed on several intermediate-scale tests. A relative ratio of 20:1 is used for the rate of production of LVRI to the HVRI production (i.e., the ratio of the rate constants of the production) in LIRIC 3.2. This ratio was assigned based on many simulations of the RTF tests performed in organic painted vessels.

The range of hydrolysis rates for organic iodides varies dramatically, ranging from negligible for iodophenol, $2 \times 10^{-8} \text{ s}^{-1}$ for CH_3I , to $1 \times 10^{-2} \text{ s}^{-1}$ for t-butyl iodide at 25°C (Wren et al., 1999a,b; Glowa and Wren, 2001). Presently, LIRIC 3.2 uses an "average rate constant" for hydrolysis of both HVRI and LVRI, based on measured rates on a wide range of organic iodides (Glowa and Wren, 2001). The hydrolysis rate at a given temperature depends strongly on the type of functional groups attached to the organic iodide, but the temperature dependence of the rate is nearly the same for various types of organic iodides. Based on this, LIRIC 3.2 assumes that the temperature dependence of hydrolysis for both HVRI and LVRI is the same as that of CH_3I .

The organic iodide model in LIRIC 3.2, using the rate constants and the partition coefficients in Table 5, reproduces results from several RTF performed in painted vessels very well (see Section 3), giving an accurate prediction of the observed gas-phase and aqueous-phase iodine speciation in addition to a reasonable assessment of the total amount of iodine in each of these phases. More work is needed, however, to determine the uncertainties of these parameters under all containment accident conditions.

2.4. Other aqueous-phase reactions

LIRIC 3.2 contains a small sub-model of representative reactions that describe the effect of trace metal impurities (such as Fe^{2+} and Fe^{3+}) on water-radiolysis products in the aqueous phase (Table 4). These reactions can be

important because they lower the concentrations of water-radiolysis species such as superoxide ($\cdot\text{O}_2^-$) and hydrogen peroxide (H_2O_2) by catalytic consumption. LIRIC model predictions (Wren et al., 1997, 2000a) indicate that the presence of these metal impurities can increase iodine volatility by over an order of magnitude at pH values greater than 6, because they inhibit the reduction of volatile I_2 by Reactions (4) and (5). Sensitivity studies on the LIRIC model, using the rate constants for the $\text{Fe}^{2+}/\text{Fe}^{3+}$ couple have also shown that there is a threshold value for concentration of metal impurities ($10^{-4} \text{ mol dm}^{-3}$ for the $\text{Fe}^{2+}/\text{Fe}^{3+}$ couple) above which there is very little additional impact on iodine volatility. Once the steady-state concentrations of $\cdot\text{O}_2^-$ and H_2O_2 become very small, the steady-state concentration of I_2 in the aqueous phase is determined predominantly by the equilibrium constant for iodine hydrolysis (Reaction (3)).

The level of trace metal impurities in the aqueous phase in post-accident containment would be reactor and accident specific and is thus a user-defined input in LIRIC 3.2. For the purposes of predicting iodine volatility, and in the absence of any information regarding the concentration of trace metal impurities, it is recommended that the limiting value ($10^{-4} \text{ mol dm}^{-3}$ for the $\text{Fe}^{2+}/\text{Fe}^{3+}$ couple) be used. This limiting value is similar to the total Fe concentration observed in the aqueous phase in RTF experiments performed in stainless-steel vessels.

2.5. Water-gas interfacial mass transfer

From a safety analysis perspective, the interest in the time-dependent concentration of gaseous iodine is due to its mobility, which gives rise to its easy transport within, and eventually outside of the containment. The main path for the production of gaseous iodine is the mass transfer of volatile iodine species (I_2 , HVRI and LVRI) from the aqueous phase to the gas phase. This is because the conversion of non-volatile to volatile iodine species occurs mainly in the aqueous phase, the media that provides the optimum conditions for volatile iodine production (Wren et al., 2000a). Water-gas-phase interfacial transfer of volatile iodine is an important process to be considered when modelling iodine behaviour in an accident.

Although the interfacial mass transfer is very important in determining gaseous iodine concentrations, accurate kinetic modelling of the process is not required. This is because under most conditions, the net rate of change of concentration of these species in the aqueous phase is slower than their interfacial mass transfer rate. Likewise, the net rate of removal of iodine from the gas phase (due to adsorption on surfaces exposed to the gas phase) would be slower than the interfacial mass transfer rate. Interfacial mass transfer that is rapid relative to the changes in masses in both phases has been observed

consistently in RTF experiments, where the mixing and flow conditions are expected to be less vigorous than those expected in containment. The fast mass transfer conditions have been observed even when sudden pH and temperature changes (which would rapidly change individual species concentrations in the aqueous phase) have been deliberately induced. Under most accident conditions, where temperature and pH changes would be more gradual, and the flow and mixing of bulk phases would be more vigorous than in the RTF, it is anticipated that interfacial mass transfer will also be fast relative to changes in species concentration. The interfacial mass transfer rate will not contribute to the rate determining step for gaseous iodine production, and a simple description of the interfacial mass transfer as a process which tries to achieve the liquid-gas-phase equilibrium (i.e., the partition coefficient) is adequate.³

Mass transfer of volatile species between the aqueous and gas phases is treated in LIRIC 3.2 by the two resistance theory, with the rate of transfer defined as in Eq. (2) in Table 5. For a given interfacial surface area and gas and aqueous volumes, the mass transfer rate of a species can be sufficiently described using two fundamental parameters: k_{MT} , the overall mass transfer coefficient and H , the partition coefficient. The value of k_{MT} depends on thermalhydraulic conditions that influence the thickness of the gas and liquid phases at the boundary layer, and has a small dependence on the nature of the species (see Eq. (4) and footnote c in Table 5). Because of its dependence on thermalhydraulic conditions, the interfacial mass transfer rate coefficient is an input parameter in LIRIC 3.2.

Fluid flows and transport properties are often difficult to characterize, therefore, for complex flow regimes such as those found in containment or in intermediate scale studies, there could be considerable uncertainty in the appropriate value of k_{MT} . However, because interfacial mass transfer is not rate determining under the conditions previously discussed, a large uncertainty in

³Further consideration should be given to mass transfer when applying the model to full size reactors. When the gas-phase volumes are large, the assumption of good homogeneous gas mixing may not be valid and a nodalized model of the gas volume in the area containing the water pool may be necessary to simulate mass transfer processes in a full-size reactor. For nodes without a water pool, the behaviour of gaseous iodine can be modelled using only Eqs. (3)–(6) in Table 5. The processes that are represented by these equations are described in Section 2.6. The choice of number of nodes and how they are used to represent the liquid gas interface will need to be determined. For the purposes of simulating RTF tests, it appears that a single node representation of the volume was adequate. Note that, if present, a condensing water film on walls is treated like another surface in contact with gas phase (see Section 2.6).

the value for k_{MT} does not result in a large uncertainty in calculating gas-phase iodine concentration.

Although the uncertainty in defining a value for k_{MT} is not critical for simulations of typical RTF experiments, the value used (ranging from 2×10^{-4} to $5 \times 10^{-4} \text{ dm s}^{-1}$ for I_2 at 25°C) (Wren et al., 2000a; Evans et al., 1990) was determined experimentally for specific flow conditions in the facility. The value $5 \times 10^{-4} \text{ dm s}^{-1}$ approaches the limiting value for transfer of I_2 across a liquid/gas interface from a pool at room temperature (Schwarzenbach et al., 1993)⁴ and is the value recommended when reliable estimates of k_{MT} are unavailable, as it will provide a conservative (bounding) estimate for gas-phase iodine concentrations under conditions where most of the iodine inventory is in the aqueous phase.

Fast interfacial mass transfer means that, at any given time, the ratio of the aqueous phase to the gas-phase concentration of a volatile species is close to the equilibrium value, H , where the partition coefficient H is defined as the ratio of the aqueous- to gas-phase concentration of a species in equilibrium. Uncertainties in the value of H will therefore have a direct consequence on the uncertainty in the calculated gaseous iodine concentration. The partition coefficient for I_2 (79 at 25°C) and its temperature dependence is well established (Wren et al., 2000a). However, there is a large range of partition coefficients for organic iodides (Wren et al., 2000a; Glowa and Wren, 2001), and this must be accounted for when modelling iodine behaviour as discussed in Section 2.3.

2.6. Surface interaction

In LIRIC 3.2, iodine-surface interactions are divided into three categories, depending on the type of surface. These are surfaces in contact with the aqueous phase ("aqueous-phase surfaces"), dry surfaces in contact with the gas phase ("gas-phase surfaces") and condensing water film on walls ("condensing surfaces").

For many accident scenarios, condensing steam and water will be prevalent in the containment atmosphere, and adsorption of iodine on dry surfaces contacting the gas phase will be less important than absorption in, or interaction of iodine with condensing films. However, for analysing many RTF and other intermediate-scale tests performed in relatively dry atmospheres, a model

for adsorption of iodine on dry surfaces is required. Adsorption and desorption is assumed to occur only for I_2 on these surfaces, because organic iodides are not readily retained on most surfaces (Rosenberg et al., 1969b). The adsorption and desorption process is formulated using a pseudo-first-order physical adsorption-desorption model (see Eqs. (3) and (4) in Table 5).

The first-order adsorption/desorption formulae given in Table 5 may be too simple to accurately describe iodine sorption on surfaces such as untreated stainless-steel surfaces (Wren et al., 1999c; Wren and Glowa, 2001). However, it is sufficiently versatile that it can be used to model adsorption on a variety of surfaces (Rosenberg et al., 1969a, b; Genco et al., 1969), assuming that the appropriate adsorption/desorption rate constants are known, and surface areas are well defined. Because they depend on plant-specific surface characteristics, the adsorption rate coefficient (or deposition velocity, k_{AD}), desorption rate constant (k_{DES}), gas-phase surface area (A_g) and volume (V_g) are user-defined input parameters in LIRIC 3.2. The adsorption-desorption rate constants used for the simulations of RTF experiments are generally taken from various bench-scale measurements. When applying an adsorption model to reactor accident conditions, it may be difficult to assign values for these parameters because of the difficulty in defining containment surface areas and characteristics properly. This problem is probably not serious for painted smooth structures whose surface area can be well approximated by using the geometric surface area (i.e., painted carbon steel).

Aqueous-phase surfaces may also retain iodine. Therefore, models for iodine adsorption on and desorption from submerged surfaces are included in LIRIC 3.2. These processes are modelled the same as the analogous processes on gas-phase surfaces with the exception that adsorption of iodide ion (I^-) and pH-dependent adsorption can also be specified.

Deposition of iodine on surfaces exposed to condensing steam is modelled in LIRIC as direct absorption on wall condensate, and is treated like iodine adsorption on dry walls, except that there is no desorption of iodine from condensate surfaces (Table 5). Iodine, once absorbed in a condensing water film, will be quickly hydrolyzed to non-volatile iodide, which will remain in the condensate (i.e., will not desorb), and be removed by gravitational drainage of the condensate into the main sump reservoir. The expression for iodine deposition on condensing film is given in Eq. (5) in Table 5, and mass transport from the condensate to the bulk aqueous phase is described as a first-order process using the rate expression is given in Eq. (6). The condensate mass transport rate depends on the rate of water condensation and therefore on the temperature difference between the gas phase and the wall, and to a minor extent on the type of surface. Three model parameters, the volume of the

⁴An upper limit of about 0.1 dm s^{-1} has been observed for the gas-phase mass transfer coefficient k_g in vigorously mixed systems without impinging flow (Schwarzenbach et al., 1993). The maximum value for the interfacial mass transfer coefficient k_{MT} for I_2 at 25°C would therefore be $1/k_{MT} = H/k_g = 79/0.1$ or $1.2 \times 10^{-3} \text{ dm s}^{-1}$ (where H is about 79 for I_2 at 25°C) if there was no liquid-phase resistance to transfer ($1/k_l = 0$). In general, k_l is an order of magnitude less than k_g .

condensate (V_{con}), the adsorption rate constant on condensing film (k_{AD}^{c}), and the volume flow rate of condensate to the bulk phase (F_{con}) are user-defined input in LIRIC. They are reliant primarily upon thermalhydraulic conditions.

3. Simulations of RTF tests

The LIRIC 3.2 model has been used to simulate RTF tests performed under wide ranges of dose rate, I^- concentration, temperature, pH, and type of surface. Only a few simulation results are presented here. LIRIC 3.2 reproduces the gaseous iodine concentration in all of these experiments within a factor of about 3 and aqueous-phase iodine concentration within $\pm 20\%$. These discrepancies are comparable to experimental uncertainties (i.e., a factor of two for total gas-phase iodine concentration and $\pm 15\%$ for total aqueous-phase iodine concentrations). The uncertainties in the gaseous I_2 and total organic iodide (HVRI(g)+LVRI(g)) measurements are estimated to be a factor of 3–5, depending on concentration distribution. The separation of HVRI(g) and LVRI(g) should be regarded as qualitative only. Because of the uncertainties in the experimental data, the ability of a model to predict the gaseous iodine concentrations observed in Radioiodine Test Facility (RTF) tests to within an order of magnitude is considered acceptable.

An earlier version of LIRIC (LIRIC 3.0), was used successfully to model irradiated solutions of CsI ($0.5\text{--}2.0\text{ kGy h}^{-1}$) in the RTF at 25 °C in stainless-steel vessels in which pH was fixed, and adjusted step-wise (Ball and Hnatiw, 2000; Wren et al., 1997, 1999a). The simulations have been repeated using LIRIC 3.2. Fig. 1 shows the simulation results for RTF test P0T2 Stage 2, in which a solution of $1 \times 10^{-5}\text{ mol dm}^{-3}$ CsI was irradiated at 1.4 kGy h^{-1} at 25 °C in a stainless-steel vessel while the pH was adjusted in controlled steps. The main objective of the test was to determine the effect of pH on iodine volatility. The simulation shows that LIRIC 3.2 models the effect of pH over the tested range (10–5) very well. LIRIC 3.2 simulations of this experiment do not differ significantly from those of LIRIC 3.0, because most of the changes made in LIRIC 3.2 deal with the effects of temperature and organic surfaces and impurities.

LIRIC 3.2 also reproduces observed results from RTF experiments performed in stainless-steel vessels at higher temperatures (up to 90 °C). A typical simulation is shown in Fig. 2 for RTF test P9T2 performed at 60 °C in a stainless-steel vessel with controlled pH steps. The modelled results are in very close agreement with those observed experimentally. (Note that calculations performed with a pH input data that more closely resembles

the experimental pH profile would improve the reproducibility.) The LIRIC 3.2 model successfully (within a factor of three for the gas-phase iodine concentration and within 20% for the aqueous-phase iodine concentration) reproduces results from several RTF tests performed in stainless-steel vessels over a wide range of pH and temperature.

The ability of LIRIC 3.2 to simulate organic dissolution, organic radiolysis and organic iodide formation in irradiated iodine solutions in the presence of painted surfaces has also been examined. The model reproduces numerous experimentally measured parameters remarkably well. Figs. 3 and 4 show the results of one of several simulations of the RTF tests in painted vessels. The simulation results shown are for RTF test P10T1, in which a solution of $1 \times 10^{-5}\text{ mol dm}^{-3}$ CsI was irradiated at 0.6 kGy h^{-1} at 60 °C in an Amerlock 400 epoxy painted vessel. The pH of the sump water was maintained at 10 for the first 75 h of the test by injections of LiOH, after which pH was allowed to drop. The pH of the sump was intentionally raised again to 10 at 280 h into the test and maintained at that value until the end of the test. Calculated values were compared with observed values for pH, total iodine concentration in the gas phase (I_2 and organic iodides), total iodine concentration in the aqueous phase, the concentration of high and low volatility organic iodides in the gas phase, and the total concentration of organic iodides in the aqueous phase. The agreement between observed and simulated results in Figs. 3 and 4 are within a factor of three for the gas-phase iodine concentrations and within 20% for the aqueous-phase iodine concentrations, which is within experimental uncertainties.

The validated range over which the LIRIC model can be applied is currently defined by the range of conditions employed in RTF experiments that have been successfully simulated. These conditions are listed in Table 6. However, because the LIRIC 3.2 model is predominantly mechanistic, the practical range of applicability of the model should be much greater than that of the tested range. For example, the water-radiolysis model within LIRIC 3.2 has been obtained and tested in studies spanning a wide range of dose rates. Sensitivity studies have shown that the steady-state concentration of the water-radiolysis species is dependent upon their primary radiolysis yield, and dose-rate independent parameters such as the concentration of oxygen, and impurities such as iodine species, trace metals and organic materials. From Sections 2.2 and 2.3, it is apparent that iodine volatility is dependent upon these water-radiolysis product concentrations and upon the aqueous pH. It follows that, as long as the relationship between water-radiolysis product concentration, pH, and iodine behaviour is well understood, and the relationship between water-radiolysis species

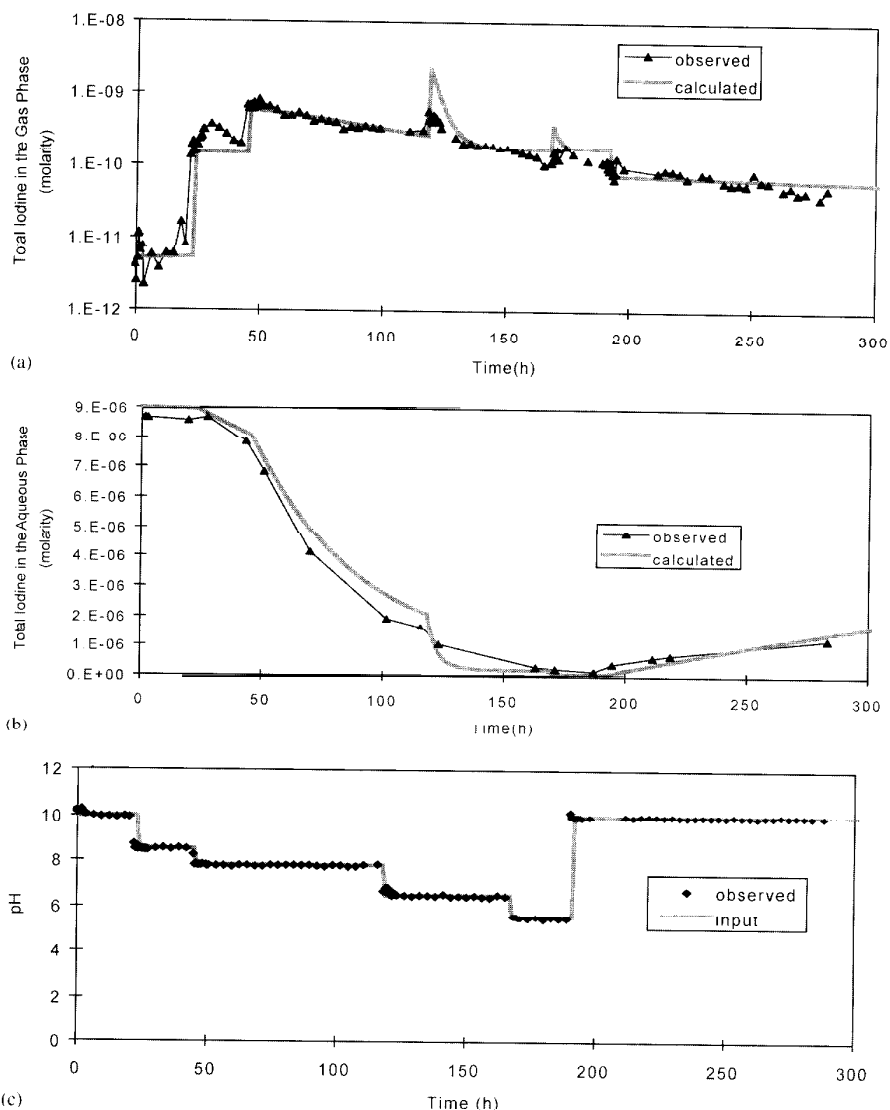


Fig. 1. Comparison of calculated versus observed concentrations of iodine (a) in the gas phase and (b) in the aqueous phase in RTF test P0T2 Stage 2 (10^{-5} mol dm $^{-3}$ CsI irradiated at 1.4 kGy h $^{-1}$ at 25 °C and at controlled pH in a stainless-steel vessel) using LIRIC 3.2. Observed pH and model input pH are shown in (c).

concentration and dose-rate well established, results calculated with LIRIC 3.2 for dose rates outside of the tested range should also be valid.

Physical phenomena, such as surface adsorption and mass transfer, are also dealt with mechanistically within LIRIC 3.2, and, therefore, there should be no effects of scale on these models. LIRIC calculations for a variety of surface areas, volumes, and surface area/volume ratios different than those of the RTF should be valid.

providing input parameters such as mass transfer and adsorption rate constants are properly chosen.

4. Summary

The LIRIC model for iodine behaviour has undergone significant revision, and now contains the components required for its use as a predictive tool in support

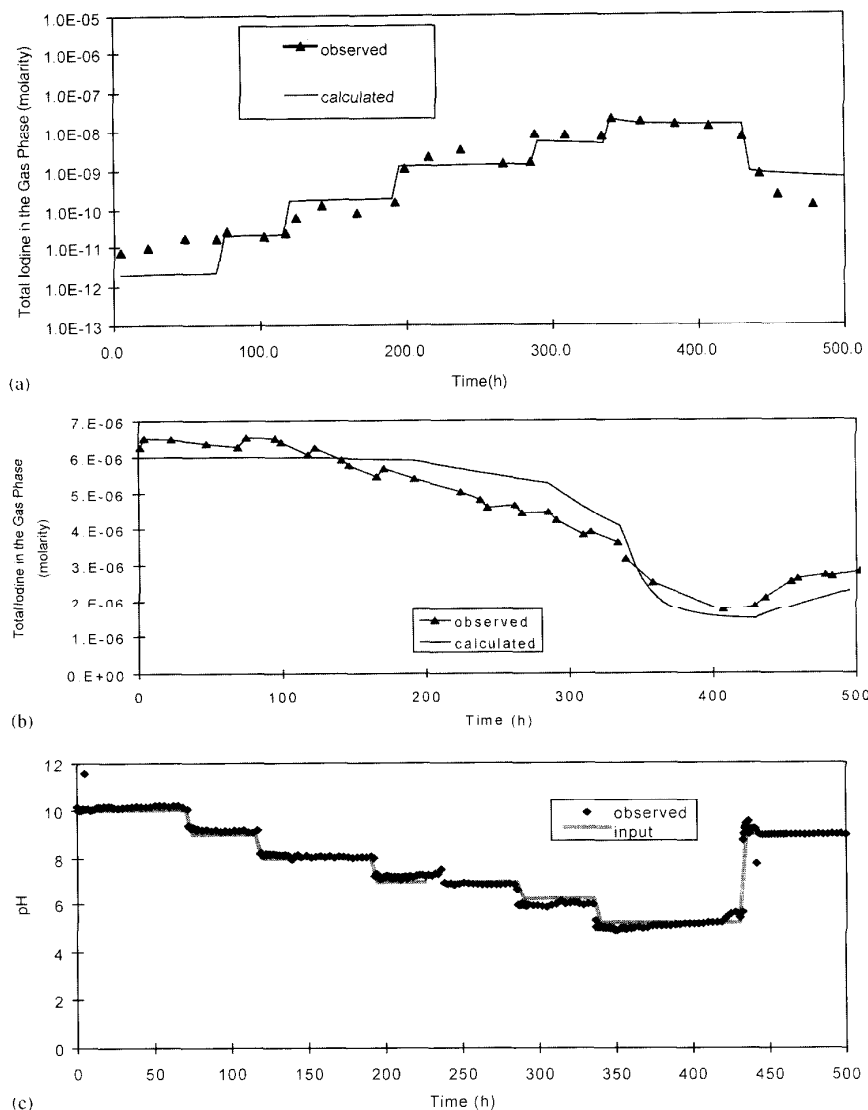


Fig. 2. Comparison of calculated versus observed concentrations of iodine (a) in the gas phase and (b) in the aqueous phase in RTF test P9T2 ($10^{-5} \text{ mol dm}^{-3}$ CsI irradiated at 0.8 kGy h^{-1} at 60°C and at controlled pH in a stainless-steel vessel) using LIRIC 3.2. Observed pH and model input pH are shown in (c).

of accident analysis. The chemical reactions and physical phenomena included in the model, now designated as LIRIC 3.2, are listed in Tables 1–5. For a given set of user-defined inputs (i.e., temperature, radiation dose, initial iodine speciation and concentration, gas- and aqueous-phase volumes, interfacial surface areas, types of surface and mass transport conditions), LIRIC 3.2

calculates the iodine concentration in the various phases (aqueous, gas, and surface), as well as the speciation (fraction of organic iodides in the gas and aqueous phases), as a function of time.

The LIRIC 3.2 model has been used successfully to reproduce intermediate-scale (RTF) tests performed under a wide range of conditions (Table 6). Some of

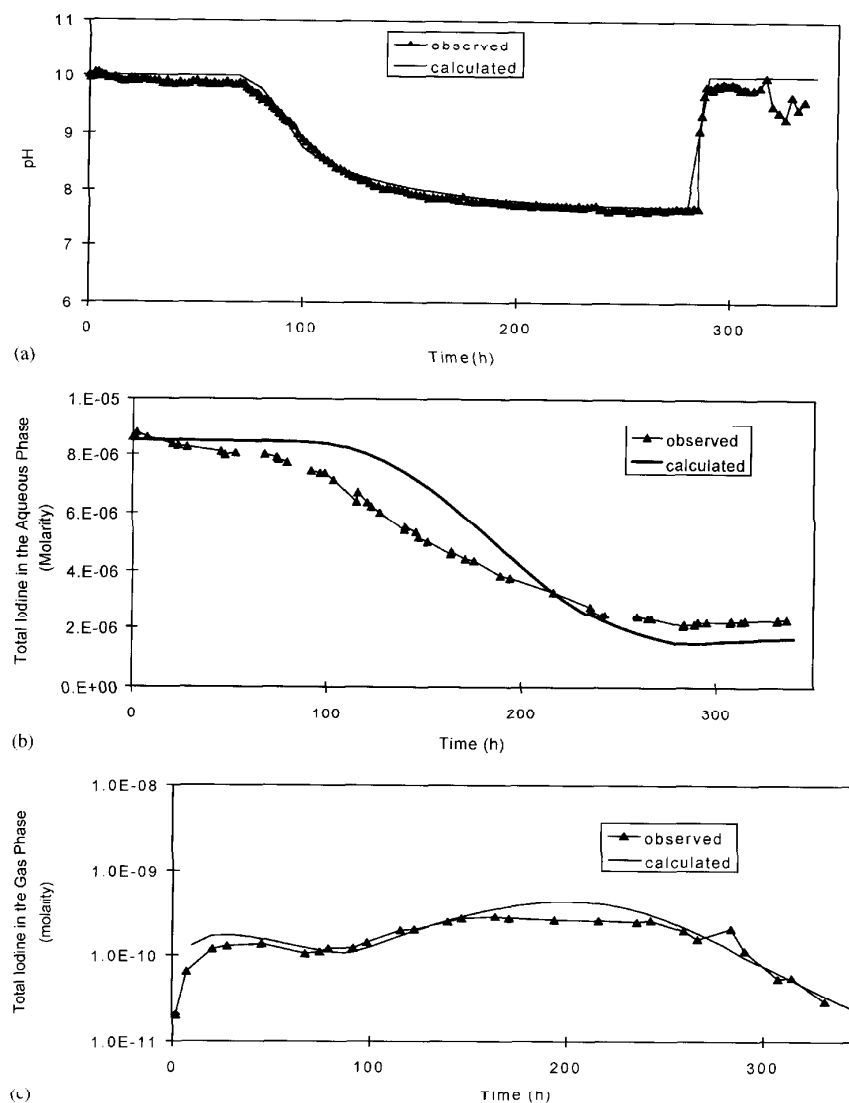


Fig. 3. Comparison of calculated versus observed values for (a) pH, (b) total iodine in the aqueous phase, and (c) total iodine in the gas phase for RTF test P10T1 (10^{-5} mol dm $^{-3}$ CsI irradiated at 0.6 kGy h $^{-1}$ at 60°C in an Amerlock 400 epoxy-painted vessel, in which pH was maintained at 10 for the first 75 h, after which the pH was allowed to drop. The pH was intentionally raised again to 10 at 280 h).

these simulation results, highlighting the effect of recent changes in the LIRIC model (i.e., the addition of temperature dependence for many of the rate constants and the addition of reactions sets for the effects of organic structural materials in containment), have been presented. The model reproduces the RTF tests within experimental uncertainties; within a factor of three for the gas-phase iodine concentration and within 20% for the aqueous-phase iodine concentration.

The area that requires further improvement in LIRIC 3.2 is the uncertainties in the effective rate constants in the organic sub-models, particularly in the sub-model for the organic iodide formation and decomposition. The organic iodide model, which categorizes organic iodides into HVRI and LVRI, uses a small number of representative reactions with semi-empirically derived rate constants and effective partition coefficients. It has shown promising results when

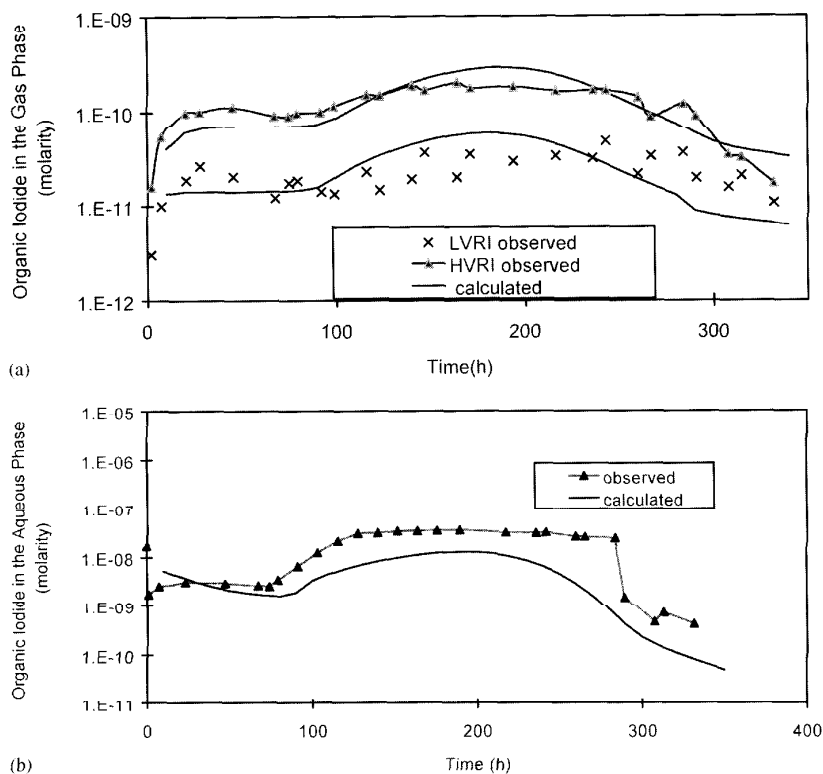


Fig. 4. Comparison of calculated versus observed values for (a) low volatility organic iodides (LVRI) and high volatility organic iodides (HVRI) in the gas phase and (b) total organic iodides in the aqueous phase for RTF test P10T1 ($10^{-5} \text{ mol dm}^{-3}$ CsI irradiated at 0.6 kGy h^{-1} at 60°C in an Amerlock 400 epoxy-painted vessel, in which pH was maintained at 10 for the first 75 h, after which the pH was allowed to drop. The pH was intentionally raised again to 10 at 280 h).

Table 6
Validated range of applicability of the LIRIC model

Parameter	Range
Dose rate	$0.5\text{--}5.0 \text{ kGy h}^{-1}$
I^- concentration	$10^{-7}\text{--}10^{-5} \text{ mol dm}^{-3}$
Temperature	$25\text{--}90^\circ \text{C}$
pH range	5–10
Surface	Steel — untreated Steel — electropolished Paint — vinyl, epoxy, polyurethane Dry or condensing water film

compared with some of the RTF tests performed in organic painted vessels. However, the uncertainties in the LIRIC 3.2 predictions under accident conditions needs to be examined. This is being addressed by

ongoing experimental and modelling programs. Successfully testing the model against additional RTF experiments, and bench-scale experiments on organic radiolysis in the presence of iodide will expand the range of conditions to which the LIRIC model can be applied with an acceptable level of uncertainties in its predictions.

The main application of LIRIC is to estimate iodine volatility in containment following an accident. For this application, it is important that the model includes sound descriptions of all the key processes. The ability of the model to reproduce several RTF experiments representing a large range of conditions is evidence that this is the case. It is also important, however, that the values of the input parameters (or boundary conditions) for the model should be well defined. For a given accident scenario, the temperature, radiation dose and initial iodine speciation in containment are defined by

upstream safety analysis calculations. Iodine modelling parameters that are not well defined in the current safety analysis are those involving surfaces, mainly:

- (a) surface areas of various surfaces,
- (b) adsorption/desorption rate constants on various surfaces, including condensing water films on walls, and
- (c) the amount and type of organic solvents available for release from painted surfaces into the sump.

There is no consistent body of data on these processes over a wide range of conditions, therefore it is difficult to narrow down the range of the values (or bounding estimates) expected in a given accident. We have performed extensive studies on the dissolution of organic solvents from various painted surfaces, and on iodine adsorption/desorption behaviour on various surfaces as a function of temperature and relative humidity. Based on these studies and the simulations of the RTF tests, values for the input parameters relevant to accident conditions have also been suggested. Work to validate these values and define their uncertainty limits under the application range intended for LIRIC 3.2 is also continuing.

5. Conclusions

Version 3.2 of LIRIC is believed to contain all the relevant chemical reactions and physical processes affecting iodine volatility in containment following an accident. LIRIC 3.2 has successfully modelled various RTF tests performed over a wide range of conditions to simulate various accident scenarios. There are still a few areas (mainly in the model's ability to predict organic iodide behaviour and in defining some input parameters), that require closer examination in order to reduce the uncertainties in applying LIRIC 3.2 to accident scenarios.

LIRIC 3.2 has been shown to reproduce the intermediate-scale test RTF results to within a factor of three for the total gas-phase iodine concentration. This is viewed as being an acceptable level of uncertainty for a containment safety code, given the uncertainties in the experimental data, and the uncertainties inherent in defining input parameters for containment conditions during postulated reactor accident conditions.

In the interests of providing a compact model for use in nuclear safety analysis, the most recent sub-models added to the LIRIC database (organic dissolution, organic radiolysis, and organic iodide formation) have employed reduced reaction sets for key processes. Because these reduced reaction sets were developed from complete mechanistic studies of the processes involved, it is hoped that the sub-models preserve the

same predictive capabilities that would have been found for the complete mechanistic models. To date, it appears that these simple sub-models perform very well for the conditions examined.

The next step in deriving a compact iodine behaviour model for safety analysis is the simplification of the aqueous inorganic iodine reaction sub-model in LIRIC (Reactions in Table 2). Extensive sensitivity analysis has indicated that the important processes dominating iodine behaviour under reactor accident conditions can be described by use of only a handful of reactions, which was discussed briefly in Section 2.2. Before it is used in LIRIC, this reduced reaction set needs to be examined for its compatibility with the other sub-models in LIRIC. The sensitivity studies, and the development and validation of a reduced version of LIRIC have been performed and are described elsewhere (Ball, 2000).

Acknowledgements

The work reported in this document was partially funded by the COG (CANDU Owners' Group) R&D Program: Working Party 06, Containment Behaviour, WPIR No. 425, 606 and 608 under the joint participation of Ontario Power Generation, Hydro Quebec, New Brunswick Power and AECL. The authors would like to thank K. Weaver at Ontario Power Generation, and G. Glowa, A. Melnyk, and D. Guzonas at AECL for providing helpful technical and editorial advice.

References

- Ball, J.M., 2000. Development of a reduced iodine chemistry subset for LIRIC. Manuscript in preparation.
- Ball, J.M., Hnatiw, J.B., 2000. The reduction of I_2 by H_2O_2 in aqueous solution. *Can. J. Chem.* (submitted for publication).
- Ball, J.M., Hnatiw, J.B., Sims, H.E., 1997a. The reduction of I_2 by H_2O_2 in aqueous solution. In: Guntay, S. (Ed.), *Proceedings of the Fourth CSNI Workshop on the Chemistry of Iodine in Reactor Safety*. Paul Scherrer Institute, Wurenlingen, Switzerland, 1996, p. 169.
- Ball, J.M., Kupferschmidt, W.C.H., Wren, J.C., 1997b. Phase 2 Radioiodine Test Facility experimental program. In: Guntay, S. (Ed.), *Proceedings of the Fourth CSNI Workshop on the Chemistry of Iodine in Reactor Safety*. Paul Scherrer Institute, Wurenlingen, Switzerland, 1996, p. 63.
- Ball, J.M., Mitchell, J.R., Wren, J.C., 2000. The kinetics of the dissolution of organic solvents from painted surfaces. Manuscript in preparation.
- Boyd, A.W., Carver, M.B., Dixon, R.S., 1980. Computed and experimental product concentrations in the radiolysis of water. *Rad. Phys. Chem.* 15, 177.
- Burns, W.G., Matsuda, M., Sims, H.E., 1990. Temperature dependence of the equilibrium constant for iodine hydrolysis at temperatures between 25 and 120°C. *J. Chem. Soc. Faraday Trans.* 86, 1443.

- Burns, W.G., Sims, H.E., 1989. The use of the FACSIMILE/ CHEKMAT program in the speciation of iodine in a PWR reactor containment following a loss of coolant accident. In: Vikis, A.C. (Ed.), Proceedings of the Second CSNI Workshop on Iodine Chemistry in Reactor Safety. Atomic Energy of Canada Limited Report, AECL-9923/CSNI-149, Toronto, Canada, 1988, p. 197.
- Buxton, G.V., Greenstock, C.L., Helman, W.P., Ross, A.B., 1988. Critical review of rate constants for reactions of hydrated electrons, hydrogen atoms and hydroxyl radicals ($\cdot\text{OH}$, $\cdot\text{O}$) in aqueous solution. *J. Phys. Chem. Refer. Data* 17, 513.
- Buxton, G.V., Sellers, R.M., 1985. Radiation induced redox reactions of iodine species in aqueous solutions. *J. Chem. Soc. Faraday Trans.* 81, 449.
- Christensen, H., Sehested, K., 1988. HO_2 and O_2 radicals at elevated temperatures. *J. Phys. Chem.* 90, 186.
- Dainton, F.S., Sills, S.A., 1962. Rates of some reactions of hydrogen atoms in water at 25 C. *Proc. Chem. Soc.* 223.
- Driver, P.A., Glowa, G.A., Wren, J.C., 2000. Steady-state γ -radiolysis of aqueous 2-butanone (MEK) and its potential impact on iodine volatility under containment accident conditions. *Radiat. Phys. Chem.* 57, 37.
- Elliot, A.J., 1992. A pulse radiolysis study of the reaction of $\cdot\text{OH}$ with I_2 and the decay of I_2 . *Can. J. Chem.* 70, 1658.
- Elliot, A.J., 1994. Rate constants and G values for the simulation of the radiolysis of light water over the range 0–300 C. Atomic Energy of Canada Ltd. Report, AECL-11073.
- Elliot, A.J., Chenier, M.P., Ouellette, D., 1990. G-values for gamma irradiated water as a function of temperature. *Can. J. Chem.* 68, 712.
- Evans, G.J., Melnyk, A., Paquette, J., Sagert, N.H., 1990. The LIRIC Database Model. In: Lawrence, S.R. (Ed.), Proceedings of the Second International Conference on Containment Design and Operation. Canadian Nuclear Society, Toronto, Canada.
- Farhataziz, Ross, A.B., 1977. Selected specific rates of reactions of transients from water in aqueous solution. III. Hydroxyl radical and perhydroxyl radical and their radical ions. US Department of Commerce National Standard Reference Data System. Report NSRDS-NBS 59.
- Furrow, S., 1987. Reactions of iodine intermediates in iodate-hydrogen peroxide oscillators. *J. Phys. Chem.* 91, 2129.
- Genco, J.M., Berry, W.E., Rosenberg, H.S., Morrison, D.L., 1969. Fission-product deposition and its enhancement under reactor accident conditions: deposition on primary-system surfaces. Battelle Memorial Institute Report, BMI-1863.
- Glowa, G.A., Driver, P.A., Wren, J.C., 2000a. Irradiation of MEK Part II: a detailed kinetic model for the degradation of 2-butanone in aerated aqueous solutions under steady-state γ -radiolysis conditions. *Radiat. Phys. Chem.* 58, 49.
- Glowa, G.A., Wren, J.C., 2001. The partitioning and destruction of organic iodides under postulated reactor accident conditions. Manuscript in preparation.
- Glowa, G.A., Wren, J.C., Degagne, G., 2000b. A generic organic radiolytic degradation model. Manuscript in preparation.
- Ishigure, K., Shiraishi, H., Okuda, H., Fujita, N., 1986. Effect of radiation on chemical forms of iodine species in relation to nuclear reactor accidents. *Radiat. Phys. Chem.* 28, 601.
- Kassai-Rabia, M., Gardes-Albert, M., Julien, R., Ferradini, C., 1993. Etude cinétique de l'action de l'eau oxygénée sur l'iode en milieu neutre ou basique. Application à la radiolyse de l'iode. *J. Chem. Phys.* 90, 801.
- Lengyel, I., Epstein, I.R., Kustin, K., 1994. Kinetics of iodine hydrolysis. *Inorg. Chem.* 32, 5880.
- Liebhaufsky, H.A., 1932. The catalytic decomposition of hydrogen peroxide by the iodine-iodide couple II and III: the rate of oxidation in neutral and in acid solution of hydrogen peroxide by iodine. *J. Am. Chem. Soc.* 54, 3449.
- Liebhaufsky, H.A., 1935. Anomalous temperature coefficients associated with aqueous halogen solutions. An explanation assuming variable hydration of the halogens. *Chem. Rev.* 17, 89.
- Lin, C.C., 1980. Chemical effects of gamma radiation on iodine in aqueous solutions. *J. Inorg. Nucl. Chem.* 42, 1101.
- Mezyk, S.P., 1996. Arrhenius parameter determination for the reaction of the oxide radical, hydrated electron and hydroxyl radical with iodate in aqueous solution. *J. Chem. Soc. Faraday Trans.* 92, 2251.
- Mezyk, S.P., Bartels, D.M., 1993. EPR measurement of the reaction of atomic hydrogen with Br and I in aqueous solution. *J. Phys. Chem.* 97, 4101.
- Palmer, D.A., Lyons, L.J., 1989. Kinetics of iodine hydrolysis in unbuffered solutions. In: Vikis, A.C. (Ed.), Proceedings of the Second CSNI Workshop on Iodine Chemistry in Reactor Safety. Atomic Energy of Canada Limited Report, AECL-9923/CSNI-149, Toronto, Canada, 1988, p. 1.
- Palmer, D.A., Ramette, R.W., Mesmer, R.E., 1984. Triiodide ion formation equilibrium and activity coefficients in aqueous solution. *J. Solution Chem.* 13, 673.
- Paquette, J., 1989. Modelling the chemistry of iodine. In: Vikis, A.C. (Ed.), Proceedings of the Second CSNI Workshop on Iodine Chemistry in Reactor Safety. Atomic Energy of Canada Limited Report, AECL-9923/CSNI-149, Toronto, Canada, 1988, p. 216.
- Poutsma, M.L., 1973. In: Kochi, J.K. (Ed.), Halogenation, in Free Radicals. Vol. II. John Wiley and Sons, New York, pp. 159.
- Rosenberg, H.S., Cromme, G.E., Genco, J.M., Berry, D.A., Morrison, D.L., 1969a. Fission-product deposition and its enhancement under reactor accident conditions: development of reactive coatings. Battelle Memorial Institute Report, BMI-1874.
- Rosenberg, H.S., Genco, J.M., Morrison, D.L., 1969b. Fission product deposition and its enhancement under reactor accident conditions: deposition on containment-system surfaces. Battelle Memorial Institute Report, BMI-1865.
- Sagert, N.H., 1989. Radiolysis of iodine in moist air: a computer study. In: Vikis, A.C. (Ed.), Proceedings of the Second CSNI Workshop on Iodine Chemistry in Reactor Safety. Atomic Energy of Canada Limited Report, AECL-9923/CSNI-149, Toronto, Canada, 1988, p. 235.
- Schwarz, H.A., Bielski, B.H.J., 1986. Reactions of HO_2 and O_2 with iodine and bromine and the I_2 and I atom reduction potentials. *J. Phys. Chem.* 90, 1145.
- Schwarzenbach, R.P., Gschwend, P.M., Imboden, D.M., 1993. Environmental Organic Chemistry. John Wiley and Sons Inc., Toronto.
- Sellers, R.M., 1986. A database for the reaction kinetics of iodine in aqueous solution. In: Deane, A.M., Potter, P.E. (Eds.), Proceedings of the Specialists' Workshop on Iodine Chemistry in Reactor Safety. Atomic Energy Research

- Establishment, AERE- R11974. Harwell, UK, September 1985, p. 91.
- Shiraishi, H., Okuda, H., Morinago, Y., Ishigure, K., 1992. Measurement on the rate of some reactions relevant to iodine chemistry in the aqueous phase. In: Ishigure, K., Saeki, M., Soda, K., Sigimoto, J. (Eds.), *Proceedings of the Third CSNI Workshop on Iodine Chemistry in Reactor Safety*. Japan Atomic Energy Research Institute, Tokai-muri, Japan, 1991, p. 152.
- Thomas, J.K., 1967. Pulse radiolysis of aqueous solutions of methyl iodide and methyl bromide. The reaction of iodine atoms and methyl radicals in water. *J. Phys. Chem.* 71, 1919.
- Vinson, J.M., 1978. Hydrolyse et transport d'iode dans l'enceinte des reacteurs a eau legere. *Commissariat a l'Energie Atomique, Institute de Protection et de Surete Nucleaire Report, SESTR-18/03*.
- Wren, J.C., Ball, J.M., Glowa, G.A., 1999a. The interaction of iodine with organic material in containment. *Nucl. Tech.* 125, 337.
- Wren, J.C., Ball, J.M., Glowa, G.A., 1999b. Studies on the effects of organic-painted surfaces on pH and organic iodide formation. *Proceedings of the OECD Workshop on Iodine Aspects of Severe Accident Management. Committee on the Safety of Nuclear Installations/Organization for Economic Cooperation and Development, NEA/CSNI/R(99)7*. Vantaa, Finland, 1999, p. 181.
- Wren, J.C., Ball, J.M., Glowa, G.A., 2000a. The chemistry of iodine in containment. *Nucl. Tech.* 129, 297.
- Wren, J.C., Glowa, G.A., 2000. A simplified model for the degradation of 2-butanone in aerated aqueous solutions under steady-state γ -radiolysis conditions. *Rad. Phys. Chem.* 58, 341.
- Wren, J.C., Glowa, G.A., 2001. Kinetics of gaseous iodine uptake onto stainless steel during iodine assisted corrosion. *Nucl. Tech.*, in press.
- Wren, J.C., Glowa, G.A., Ball, J.M., 1997. Modelling iodine behaviour using LIRIC 3.0. In: Guntay, S. (Ed.), *Proceedings of the Fourth CSNI Workshop on the Chemistry of Iodine in Reactor Safety*. Paul Scherrer Institute, Wurenlingen, Switzerland, 1996, p. 507.
- Wren, J.C., Glowa, G.A., Merritt, J., 1999c. Corrosion of stainless steel by gaseous iodine. *J. Nucl. Mater.* 265, 161.
- Wren, J.C., Jobe, D.J., Sanipelli, G.G., Ball, J.M., 2000b. Dissolution of organic solvents from painted surfaces into water. *Can. J. Chem.* 78, 464.
- Wren, J.C., Paquette, J., Sunder, S., Ford, B.L., 1986. Iodine chemistry in the +1 oxidation state. ii. a raman and uv-visible spectroscopic study of the disproportionation of hypoiodite in basic solutions. *Can. J. Chem.* 61, 2284.
- Wren, J.C., Sagert, N.H., Sims, H.E., 1992. Modelling of iodine chemistry: the LIRIC database. In: Ishigure, K., Saeki, M., Soda, K., Sigimoto, J. (Eds.), *Proceedings of the Third CSNI Workshop on Iodine Chemistry in Reactor Safety*. Japan Atomic Energy Research Institute, Tokai-muri, Japan, 1991, p. 381.